DOE/ET/03425-20

MEASUREMENT OF AIRBORNE RADIOACTIVITY AND ITS METEOROLOGICAL APPLICATION

Part VIII

by

R. Reiter, H.-J. Kanter, R. Sládkovič, H. Jäger

and

K. Pötzl

Fraunhofer-Institut für
Atmosphärische Umweltforschung

D-8100 Garmisch-Partenkirchen
W-Germany

Annual Report
1st August 1976 through 31st October 1977

U.S. Department of Energy
Agreement No. DE-ACO2-76EV 03425

formerly EY-76-C-02-3425, Mod. 8

December 1980

DISCLAIMER

DOE/ET/03425-20

MEASUREMENT OF AIRBORNE RADIOACTIVITY AND ITS METEOROLOGICAL APPLICATION

PART VIII

by

R. Reiter, H.-J. Kanter, R. Sladkovic, H. Jäger
and
K. Pötzl

Fraunhofer-Institut für
Atmosphärische Umweltforschung

D-8100 Garmisch-Partenkirchen
W-Germany

ANNUAL REPORT

1 August 1976 through 31st October 1977

U.S. Department of Energy
Agreement No. DE-ACO2-76EV03425
formerly EY-76-C-02-3425, Mod.8

December 1980

Table of contents

page

page

I. OBJECTIVES AND ACTIVITIES OF REPORTING PERIOD

1. General

The basic elements for the current investigations have been detailed in previous reports (Parts I - VII).

Activities performed during the reporting period served to solve the following problems:

a) Detection of intrusions of stratospheric air into the troposphere through observing the time variation of the concentration of cosmogenic radionuclides (e.g. Be7, P32, P33).

b) Calculation of isentropic trajectories for the influx of air masses to the measuring site Zugspitze for selected long-term periods aimed at a characterization of the tropospheric flow processes.

c) Establishment of a climatology of the stratospheric-tropospheric exchange.

d) Installation of an ozone measuring network with stations at different levels of the lower troposphere.

e) Monitoring of stratospheric aerosol layers.

d) Study of the influence of solar events on the stratospheric-tropospheric exchange.

2. Characterization of Particulars, Objectives, and Activities During the Reporting Period

The reporting period includes specifically actions to:

2.1. Data Sampling and Processing

Aerosol sampling at the peak of the Zugspitze, chemical treatment of filters and radiochemical analysis of samples

were continued. To ensure the planned climatological processing of radionuclide data, utmost care was paid to to the calibration of the course of analysis and the measuring systems.

2.2. Recording of the Tropospheric Ozone

Ozone recordings at the Zugspitze were continued. In addition, ozone stations Wank (1780 m ASL) and Garmisch (700 m ASL) could be installed.

2.3. Monitoring of Stratospheric Aerosol

Routine monitoring of the stratospheric aerosol could be started. Extension of the lidar system needed for this is practically concluded.

2.4. Correlation Between Stratospheric Intrusions and Solar Events

The correlation between stratospheric intrusions and solar events has been studied according to the key day method using an 8-year measuring series of stratospheric radionuclides.

II. GENERAL METHODS OF STUDY

The methods of study described in previous reports were retained. No problems arose in their application.

III. PRACTICAL EXECUTION OF LABORATORY PROCEDURES

1. Sampling, Chemical Analysis, Physical Methods

Aerosol sampling at Zugspitze peak and radiochemical processing of filters for determining the concentration of stratospheric radionuclides Be7, P32, and P33 were continued without any change. No problems were encountered.

2. Measurement of the Tropospheric Ozone

Ozone measurements at the Zugspitze were resumed after a longer interruption in October 1976. During the interruption the measuring device was overhauled and improved. At station Zugspitze a new suction pipe was installed. The aspiration area was installed at some distance of the building through a cantilever and is above the precipice in free ventilation. Eventually possible influences through the building on the ozone measurements have thus been excluded. A heated dome at the pipe intake guarantees proper function even under wintertime operating conditions. Heating is regulated automatically as a function of air temperature surrounding the suction dome. The suction pipe consists of a teflon tube having a 10 mm inner diameter and is rinsed through a membrane pump with about 300 l air per hour.

In October, the measuring stations Wank (1780 m ASL) and Garmisch (740 m ASL) could be put into service. Thus, all necessary requirements for measuring the balance of the tropospheric ozone discussed in Annual Report Part VII have been realized.

3. Trajectory Analysis of Tropospheric Flow Processes

As described previously, two selected long-term periods (20 February - 25 May 1974 and 20 July - 20 September 1974) are used to study the climatology of stratospheric intrusions and the associated flow processes in the troposphere. The isentropic trajectory analysis needed for that are largely concluded. The results and conclusions will be presented in Annual Report Part IX.

IV. GRAPHICAL REPRESENTATION OF FALLOUT, COSMOGENIC RADIONUCLIDES, AND O_3 AT THE ZUGSPITZE FROM 1 AUGUST 1976 THROUGH 31 OCTOBER 1977

Fig. 1 represents the time variation of the concentration of fallout and cosmogenic radionuclides Be7 and P32. The daily means of the ozone concentration, measured at the Zugspitze, are plotted in the lower section.

As far as fallout is concerned, steep increases (indicated by .... , use scale on the right side) after the Chinese nuclear tests on 25.09.76 and 17.09.77 are clearly evident. Remarkable is also the rise in the concentration during the summer half-year May - August 1977. This coincides with an increase in the mean ozone concentration from some 25 to 40 ppb. The Be7 and P32 values show in contrast no obvious annual variation. The concentration peaks produced by stratospheric intrusions are superposed on an almost constant background level. Especially striking events were observed in October and December 1976, in March and at the end of May 1977.

Stratospheric intrusions produce in ozone time-coinciding peaks of relatively small amplitude superposed on the above mentioned steady ozone trend. These observations suggest that here two independent phenomena overlap each other. The gradual change in the ozone concentration coinciding with the fallout concentration corresponds to the classical conception according to which the influx of stratospheric ozone into the troposphere leads to an elevated background level there in the summer months. Stratospheric intrusions lead, in contrast, to a short-time ozone increase independent of the season. Therefore, it may be assumed that ozone influx into the troposphere as a result of stratospheric intrusions makes just a relatively small contribution to the tropospheric ozone balance.

V. OBSERVATION OF STRATOSPHERIC AEROSOLS BY LIDAR

1. State of the Lidar System

The present state of the lidar system, the computer control of all functions of the emitter and receiver electronics, the range gate technique, which allows a backscattering profile with reasonable height resolution to be obtained with the 10-channel photon counter, and the final off-line data evaluation have been described in detail in the last Annual Report (June 1978) and remained unchanged during the period covered by this report.

Routine probing of the stratosphere has been taken up in October 1976 after replacing the EMI 9816 by an RCA 8852 photomultiplier. This new PMT is distinguished by a much better time resolution resulting in better precision of the counting data and increased range of linear response.

The installation of a filter revolver in the receiver light path (which replaces the grey wedge , described in the last report) holding several neutral filters and providing unattenuated light passage and light attenuation at several levels simplifies the reconstruction of a backscattering profile, because fixed attenuation factors can now be incorporated in the program.

At present a backscattering profile is recorded by observing 600 m intervals per channel of the 10-channel counter and 7 successive delay settings are necessary to cover a height interval from 7 to 40 km. Per delay setting laser returns are recorded until a 4% standard deviation of the counting rate is obtained but a maximum of 50 laser firings per delay is not exceeded. Up to 4 series per night averaged provide a mean profile which consists then of as much as 1000 to 1200 individual laser returns.

2. Raylcigh Backscatter Profiles

The measured total backscattering (i.e. molecular plus particulate backscattering) has to be compared with the backscattering from a purely molecular atmosphere (Rayleigh scattering). To minimize errors we try to combine measured backscattering profiles with Rayleigh profiles derived from actual atmospheric density data which are produced by our own radiosondes. These radiosondes are launched at the site of the institute at least within 12 hours from a lidar campaign.

In case radiosonde data cannot be made available a "standard" profile has to be taken as reference. To check on the validity of such a "standard" profile, 37 Rayleigh profiles obtained from radiosonde data between January 1975 and May 1977 have been examined. This material has been investigated regarding seasonal trends and the backscattering profiles have been classified as follows: Below the tropopause (height interval 0 - 8 km) and above the tropopause (height interval 20 - 30 km) the slopes of the profiles have been determined and related to the time scale. Below the tropopause, which usually is found between 10 - 13 km, a seasonal trend of the inclination is found with a maximum in June - July and a minimum in December - January, however the scatter of the data is in the order of the seasonal variations. Only little seasonal variations can be found above the tropopause with a scatter by far exceeding the variations. So any slope of the profile can be found at any time.

Applying a seasonal "standard" Rayleigh profile if actual radiosonde data are not available therefore is only a compromise. Deviations of the actual Rayleigh profile from a "standard" profile can be in the order of the presently measured net aerosol backscattering.

Our Rayleigh profiles have been compared with the Rayleigh profile derived from density values of the 1976 US Standard Atmosphere. Below the tropopause there is very good agreement, the "US Rayleigh profile" showing a slope corresponding to our mean value of all evaluated profiles. Above the tropopause the "US Rayleigh profile" shows a steeper slope. However, the scatter of our profiles includes the slope of the "US Rayleigh profile" above the tropopause.

3. Measured Backscattering Profiles

Intense instrumental maintenance now allows to make use of almost all clear sky periods. Unfortunately the number of nights suitably clear is rather limited and we are forced to conduct our measurements during nights when cirrus clouds tend to hamper our recordings. Only during night time measurements can be performed to avoid the high background due to diffuse sky radiation. Cirrus clouds, usually changing rapidly in density, can cause an intensity shift of the individual sections of the backscatter profile and matching of these sections with the general trend of the whole profile might then be necessary.

During the period October 76 through October 77, 22 backscattering profiles, in most cases up to 35 km and more, have been recorded, many of them through a more or less dense cirrus layer. Two of these profiles are shown in Figs. 2 and 3. The polygonal curves are the measured total backscattering, the smooth curves the calculated molecular backscattering. The horizontal bars denote 1 standard deviation of the statistical fluctuations of the photon counts.

The matching of the measured total backscattering signal with the calculated molecular return is accomplished at height levels with minimum aerosol backscattering. Suitable levels are above the tropopause around 15 km and between

20 and 25 km. Deviations from the purely molecular backscattering are genererally found around the tropopause if cirrus layers are present, between 16 and 22 km, and above 25 km.

On February, 14 July 24, September 15 and 30 (Figs.2 and 3), and October 12 and 30, 1977, the degree of depolarization of the return signal (ratio of perpendicular to polarized returns, with respect to the plane of polarization of the outgoing laser pulse) has been determined. In the figures the depolarized return is shown, which due to reduced intensity can be observed only from altitudes up to 20 to 23 km. Returns from cirrus clouds yield depolarization degrees of 3 to 54%. The depolarizing effect of the molecular atmosphere is 2.5%, and the same value has been determined for the aerosol layer. This would point at a spherical shape of the aerosol particles in the lower stratosphere.

4. The Stratospheric Aerosol Layer

A good means of describing particulate backscattering is the scattering ratio, i.e. the quotient of measured total backscattering to calculated molecular backscattering. Figs. 4 and 5 present 22 vertical profiles of the scattering ratio from the time period October 1976 to October 1977. Each curve is the mean of several individual profiles recorded during the night of observation. The tropopause level (denoted by T in the graphs) usually is found at 10 to 12 km where in many cases cirrus clouds produce large scattering ratios. Above the tropopause a distinct layer of increased backscattering intensity in the order of 10 to 15 % of the molecular return can be observed. The lower boundary of this layer is found between 13 and 16 km, the upper boundary between 22 and 26 km. Maximum backscattering is recorded between 17 and 22 km. The ratio values correspond with those

reported for the pre-Fuego situation. The eruption of the volcano Fuego in Guatemala in October 1974 was the last major volcanic injection into the stratosphere.

Towards higher altitudes above 25 km the scattering ratio in many cases is again rising. But the error margins do not allow the discussion of possible aerosol layers at higher altitudes.

5. Error Discussion

The 1 σ square root error of the photon counts amounts to about $\pm$2% at 10 to 15 km and increases to about $\pm$7% at 30 to 35 km. The Rayleigh profile derived from radiosonde density data is affected by the radiosonde uncertainty, but by matching calculated and measured backscattering profiles this error will be reduced and the remainder will not exceed 1 or 2 %. In some cases the Rayleigh profile has to be extrapolated to higher altitudes causing an error of the same order. For the calculation of the Rayleigh backscattering profile particulate extinction has been disregarded. The error thus introduced has been estimated applying literature values of the particulate backscatter to extinction ratio to an assumed aerosol layer between 18 and 25 km. An error of .2% of the two-way transmission caused by this layer has been calculated and can be neglected. Thus a maximum error of about 10% can be assumed for our measurements between 30 and 35 km, and about 4% at the height of the aerosol layer.

VI. NEW RESULTS REGARDING THE INFLUENCE OF SOLAR ACTIVITY ON THE STRATOSPHERIC-TROPOSPHERIC EXCHANGE

Summary

The dependence of stratospheric intrusions on solar events is analyzed on the basis of 8-years' recordings of the concentration of stratospheric radionuclides and the ozone at 3 km altitude as well as of the total ozone.

A significant, even though weak influence of solar magnetic sector structure boundaries of type -/+ can be identified, a seasonal influence is also observed, however.

The strong 50 to 80% increase in the frequency of stratospheric intrusions after solar H_α-flares is significant and completely independent of the phase of the solar cycle and season. The total atmospheric ozone shows also a correlation with solar flares: A well defined maximum on the day preceding the flare. The neutron density clearly shows the Forbush decrease on the H_α-key day. Using key days with Forbush minimum for the superposed epoch analysis reveals a significant maximum of the Be7-concentration on the day before the flare (rise by about 45 to 60%).

Noteworthy is the following sequence: Approximately 3 days before the solar flare the neutron density begins to decease, 1 - 2 days before the flare the total atmospheric ozone maximizes, and 2 to 3 days after the flare we find the maximum of the Be7 in the troposphere as a consequence of the stratospheric intrusion.

1. Introduction

In a previous publication we provided the results of a 5-year investigation into the dependence of the stratospheric-tropospheric exchange on solar activity [1].

This study yielded positive results, in particular it was possible to identify an increase in the frequency of stratospheric intrusions after solar flares and interplanetary magnetic sector structure boundary passages. Yet, some questions remained open regarding not only the extent to which these results might be generally improved by extending the data records over a still longer period of time, but also the influence that the phase of the solar cycle might have on the correlations, and finally some reflections on a conceivable causal chain.

We continued therefore our studies and classified the data according to the previous but also to more recent aspects. Observations covering 8 years are available now, that means a period comparable to the solar cycle.

For this reason it was possible to subdivide the total period into the following 3 phases of solar activity beginning at the end of 1969 (the time sections stated below include in each case the years mentioned):

a. Period of maximum solar activity from November 1969 through 1972 (abbr. in the figures SOLAR MAX)

b. Period of decreasing solar activity in the years 1973 through 1975 (abbr. in figures SOLAR DECR)

c. Period of minimum solar activity in the years 1975 through 1977 (abbr. in figures SOLAR MIN[+]).

In view of the multitude of data we made an additional subset of the entire records according to seasons where after careful considerations the respective periods winter/spring and summer/fall have been compiled.

[+]) The year 1975 appears in both period 2 and period 3 since drawing a sharp line between b and c neither was possible nor meaningful

In considering the stratospheric-tropospheric exchange, the seasonal influence cannot be disregarded and therefore a season-dependent effect of solar events might be conceivable.

Special emphasis has been on the question as to what extent a correlation can be established between the Forbush decrease (e.g. the reduction of the energy density of the galactic cosmic rays in the lower atmosphere) and the stratospheric-tropospheric exchange. This study is linked to some reflections on a possible causal relationship.

Finally, some isolated events of stratospheric intrusions have carefully been analyzed including all relevant data. In this connection also ozone-radiosonde profiles have been taken into account and just as well measurements of the atmospheric total ozone.

Now as in the past the discussion of statistically obtained results implies the question of how a stratospheric intrusion may be triggered. There is certainly no doubt that according to Mahlman [2] the sinking motion of the stratospheric air is to be associated with a cyclogenesis. Extensive investigations at our institute into the meteorological conditions within the region of and during the stratospheric intrusion confirmed this conclusion. However, the manner in which such a cyclogeneses is triggered remains still an open question. We may assume that for this to happen rapid temperature changes in the lower stratosphere - though only to a least extent - might suffice to upset a labile condition and thus initiate the event of an intrusion. In this light,the variations in the concentration of ozone are of great interest as they possibly constitute an essential link in a causal chain. That's the reason why we pay particular attention to the ozone profiles. It should however be mentioned at this point that only profiles which have been obtained in rapid

time succession - minimum interval one day - can be of interest here. Ozone radiosonde flights of our own have shown, for instance, that the ozone profile undergoes frequently rapid variations even from day to day.

As a new aspect we considered also the reliability of the daily weather forecast issued by the German Weather Service and that for the following reason: As mentioned before, we assume that the triggering of a cyclogenesis and an intrusion of stratospheric air occurs very quick through activation of a labile atmospheric condition. Obviously then, the forecasting accuracy around such an event is reduced. Aside from that, such investigation is also of practical concern: The question arises as to what extent consideration of solar activity and its predictable variations may provide an additional parameter for improving the verification rate of weather forecasts.

Some of the results reported in this study have been presented for discussion at the Symposium/Workshop "Solar Terrestrial Influences on Weather and Climate" July 1978, Columbus, Ohio [3].

2. Data

As outlined in [1], we use for the identification of stratospheric intrusions both the concentration of Be7 (further P32 and other radionuclides) measured over each 24-hour period at our observatory Zugspitze at 3 km altitude and the concentration of the local ozone recorded at the same station. The ozone profiles are obtained with our radiosonde. It delivers the ozone concentration (with an ECC-ozone meter) and all other meteorological data up to an altitude of at least 35 km (apart from exceptions). Recently, we have begun to perform measurements of our own of the atmospheric total ozone with a Filter Ozone Spectro-

photometer [4] but this instrument is available for about one year only. Irrespective of that, we use the total ozone data from the stations Arosa and Hohenpeissenberg (we are especially grateful to H.W. Dütsch and W. Attmannspacher for providing these data).
Statements regarding the significance of weather forecasts were drawn from the periodic information of the German Weather Service.
All other geophysical data such as solar flares, geomagnetic activities, neutron densities, solar flux, radio propagation, and others were obtained from the Solar-Geophysical Data issues of NOAA [5].
We give our special thanks to J.M. Wilcox for providing the data of the sector structure boundary passages. Statistical processing of data was done by superposed epoch analysis (refer to [1] for particulars) using in each case a period of 12 days before to 12 days after the key day.

The vertical bars in the diagrams show now as before the standard deviation for an assessment of the statistical evidence.

3. Results of the Superposed Epoch Analysis

3.1. Passages of Solar Magnetic Sector Structure Boundary as Key Days

The augmentation of data records based on the now extended period of observation led, surprisingly enough, not to an improvement of the earlier noted correlation between the concentration of the Be7 (as indicator for the frequency and intensity of stratospheric intrusions) and the sector structure passages. Fig. 6 shows the essential result. We will consider right here the dependence on the season. The two diagrams on the left apply to winter and spring, the right ones to summer and fall. Viewing only sector passages

of type +/- (see [1] for details) we observe practically no correlation, at least not for the seasons winter and spring. (Around the key days during summer and fall we find periodic variations which, however, do not reveal a meaningful correlation to the key day itself). If the analysis is restricted exclusively to the period of maximum solar activity, the increase in the Be7 concentration persists on the average after the key days. During minimum solar activity this correlation vanishes as shown by our most recent evaluations.

Viewing sector passages of type -/+, a correlation persists even with the use of the entire data records covering eight years as can be seen from Fig. 6. However, on the key days we find surprisingly a maximum in winter and spring but a minimum in summer and fall. In that, our latest results are not at variance with our earlier findings [1]. But here, too, it holds that during the period of minimum solar activity the sector structure passages cannot be regarded as affecting significantly the frequency of stratospheric intrusions.

The result of this analysis shows that augmentation of the data does not necessarily lead to a confirmation of our findings but it refines the picture of the correlations under study. Separate handling of the seasons and sector polarities is therefore an absolute requirement. After a further extension of data we will treat separately the four seasons, too.

Additional results of a data analysis based on sector structure passages are mentioned only in brief:

a) A breakdown of all data according to polarities of sectors and seasons winter/spring and summer/fall does not reveal a convincing correlation.

b) An analysis of the total ozone yielded a very pronounced and significant maximum 2 days after the sector passage of type +/- in winter and spring. This is a tentative result and must be confirmed by additional data.

3.2. Solar H_α-Flares as Key Days

The definition of flares which have been used in our studies was the same as before ([1]), importance ≥1, occurrence between 20^oW and 20^oE of heliographic length. Fig. 7a shows that the earlier findings regarding the Be7 concentration, i.e. the frequency and intensity of stratospheric intrusions are confirmed in every respect. The maximum 2 to 3 days after the key day is not only observed with the entire material but also for each phase of solar activity, even during its minimum. The amplitude of the variation is practically the same over all 4 phases of solar activity and, indeed,it slightly rises with increasing solar quiet (rise by about 50% during maximum or 80% during minimum solar activity). The variations of indicator Be7 on the key day (or shortly before) until the 2nd or 3rd day thereafter are clearly evident irrespective of the data group.

Fig. 7b shows that the correlation between Be7 - i.e. the stratospheric intrusions - and H_α-flares is not dependent on the seasons either. Thus, we are facing here a stable and fundamental process which is independent of the phase of solar activity and the change-over of seasons.

The bottom line in Fig. 7a denotes the quotient P32/Be7 around the H_α-flare key days. We observe a correlation between this quotient and the flares: At the time of solar maximum the quotient is found to maximize on the key day, and at times of solar minimum it is at a minimum on the key day. If we simultaneously consider the seasons, we note (in reasonable agreement with [1]) the following:

In winter and during solar minimum the quotient declines on the key day to about 20 x 10^{-3}, in summer and during solar maximum it rises to 65 x 10^{-3}. The former value means a residence time of the aerosol in the lower stratosphere in the order of 50 to 70 days, the latter quotient such one of 15 to 20 days. Accordingly, solar activity - especially solar flares - seem to influence significantly the residence time of stratospheric aerosols.

Fig. 8 shows in the upper line the behavior of the ozone concentration at 3 km altitude and in the second line the variations of the atmospheric total ozone before, during, and after solar flares. The concentration of the local ozone at 3 km altitude increases significantly from the 3rd day before the flare until the 5th day thereafter. At the time of solar minimum a significant change cannot be seen but in this case the number of data is still too small.

Notable is the behavior of the atmospheric total ozone: We find a significant decrease from the day preceding the flare which continues until the 4th or 5th day following the flare. The amplitude reaches at the time of decreasing solar activity almost 10%. During minimum solar activity, however, such a correlation is no longer observed (only 26 key days).

Since the question of an influence of solar activity on the atmospheric ozone has been discussed for many years, these results should be judged from another aspect. They possibly may be of importance with regard to a causal link which we will specify later.

Fig. 9 shows the correlation between solar flux (2695 MHz) and the neutron density, respectively, with H_α-flares. The solar flux responds in a known manner: A broad maximum on the flare day, increase and decrease extending over several days. With decreasing solar activity the mean value of

the solar flux shows also a marked decline. The amplitude of the variation is almost independent thereof, however.

The neutron density clearly reflects the well defined Forbush decrease: Attenuation of the galactic cosmic rays by the solar wind, an event setting in a few days before the flare does actually occur. The minimum of neutron density is found approximately on the 4th or 5th day after the flare. The mean value of the neutron density increases, as is known, continously with decreasing solar activity. It is remarkable that the amplitude of the variation around the flare key days is rather greater during the period of solar minimum than during that of solar maximum. This is certainly due to the fact that during solar minimum the flare events occur well isolated in time which results in optimum synchronization by the superposed epoch analysis method.

The flare-related variations of the neutron density are significant. The fact, that reduction of the neutron density sets in several days before the flare, i.e. as an active region (M-region) approaches the central meridian of the sun needs explicitly to be pointed out again. Without providing a figure as proof it is merely mentioned here that the relative sunspot number and also the calcium plage index show similar to the solar flux a broad maximum during the period of H_α-flares, and they are also characterized by an increase extending over 5 to 7 days until the flare event.

3.3. Days with Maximum Forbush Decrease as Key Days

Using the daily means of neutron density we selected days with a maximum Forbush decrease (i.e. minimum of neutron density). Fig. 10 shows in the bottom line the variation of neutron density around these key days.The principle of selection is thus clearly presented: Minimum of neutron density on the key day or on the 1st day thereafter, steep

decrease of the neutron density toward the key day, beginning decrease of the neutron density between 2 - 5 days prior to the key day. It is also interesting to note in Fig. 10 the behavior of solar flux around the Forbush key days: Absolutely independent of the phase of solar activity the maximum of solar flux is found 3 days before the key day.

Fig. 11 illustrates the behavior of geomagnetic index Ap and the index of radio propagation around the Forbush key day. Ap shows the maximum on the key day but the increase sets in several days before. The radio propagation index decreases on the average 5 to 6 days before neutron density, reaching it maximum on the key day. Figs. 10 and 11 shall give particularly clear evidence of the well defined and meaningful relation of the selected Forbush key days and the solar behavior.

Fig. 12 relates the stratospheric intrusions Be7 as indicator) and the stratospheric residence time (quotient P32/Be7) to the Forbush key days. The total data and the data covering the period of maximum solar activity show with statistical evidence that the Be7 reaches a maximum on the day before the Forbush key day. Consequently, stratospheric intrusions occur very often 2 to 3 days before the key day. The quotient P32/Be7 reaches its minimum with about 35×10^{-3} on the Forbush key day. Prior to the Forbush key day the quotients are - even though fluctuating - essentially higher. That means, that a correlation exists also between the Forbush effect and the residence time of aerosols in the lower stratosphere. The number of key days during decreasing or minimum solar activity was too small to obtain significant results (N = 10 - 18). Gathering of more material is therefore required.

The amplitude of the variation of the Be7 concentration from the 7th until the 1st day before the Forbush effect

is in the order of 45 - 60%, that means it is analogous to the variation around H_α-flares.

It remains to be mentioned that also the relative sunspot number and the calcium plage index show a characteristic variation around Forbush key days, with the maximum occurring 1 to 3 days before the Forbush effect.

The mentioned correlation between stratospheric intrusions and stratospheric residence time, respectively, and the Forbush effect may possibly be regarded with a view to a causal link which we will discuss in some detail later.

3.4. Days with Maximum Be7 at 3 km Altitude as Key Days

From the hitherto existing results we should expect that solar or geophysical parameters would show a variation if days with maximum Be7 concentration are taken as basis for a superposed epoch analysis. We must consider, however, that not every maximum in the Be7 concentration is caused by a solar event. Such a maximum may have also purely meteorological causes: Washout, for instance, removes the Be7 from the troposphere and a Be7 peak may therefore occur between two washout periods. Fig. 13 shows some results from the total data. We find that the neutron density and atmospheric total ozone decrease significantly from the 2nd day before the key day until the 2nd day thereafter. That is consistent with our earlier findings. The noted neutron density variation corresponds to the typical trend of the Forbush effect which is associated with a maximum of the Be7. Thus, the time lapse in Fig. 13 is in full agreement with our above stated findings. The same applies to the total ozone: It is clearly reduced after the solar flare (Fig. 8), that means at a period when the maximum of the Be7 is found (Fig. 7a).

Finally, Fig. 13 shows that the Be7 peak at 3 km altitude is

also associated with a maximum of the local ozone concentration. This, again, is a logical consequence because in the case of intrusions the ozone flows from the stratosphere into the tropospheric station just so as the Be7.

3.5. A Conspicuous Sequence

Fig. 14 compiles the dependence of neutron density, total ozone, and Be7 on solar H_α-flares where we purposely confine ourselves to the period 1973 through 1975. Although solar activity decreased during that period and the individual flares occurred well isolated in time, the total number of flares was not too small for a statistical investigation (number of cases: 50). We observe an interesting sequence: As soon as the neutron density starts to decrease (1. in a), the total ozone reaches temporarily a maximum (2. in b), and 4 to 5 days later the maximum of the Be7 is found (3. in c). Certainly it is not possible to infer from that immediately a physical link. Nevertheless this time sequence gives us a thought: It appears as if the triggering process for a stratospheric intrusion would be initiated by 1. and 2., so that then, after a travel time of 4 to 5 days, the maximum of the Be7 can be observed at 3 km altitude. Anyway, this sequence is a stimulus to a future detailed study of the time variations of the 3 afore mentioned parameters with particular consideration of the fine structure of the ozone concentration up to at least 35 km.

4. Conclusions and Discussion of the Recent Relevant Literature

It seems to be interesting that already with the use of an 8-year data material it has been possible to identify a significant influence of solar activity on atmospheric conditions and processes (stratospheric intrusions). The most obvious correlation is found with H_α-flares irrespective of

solar activity and seasons. Compared with this, the correlation between passages of the sector structure boundary and stratospheric intrusions is much less pronounced at specific seasons and during minimum solar activity. Incidentally, there are more recent investigations (see e.g. [6]) which cannot confirm earlier findings regarding effects of sector structure boundary passages in the atmosphere (c.f., however, also [7]).

When discussing solar influences on weather and climate we must strictly distinguish between long-term relationships (see, for instance [8]) and short-term phenomena. The latter type applies to time lapses extending over periods in the order of days or weeks (see e.g. [9, 10]) and the other one to trends in the order of one or more solar cycles. Our investigations discussed in this paper belong to the type of short-term phenomena although the data records used cover a period of 8 years. New findings concerning both types of the solar terrestrial relationship have been presented at a Symposium/Workshop in 1978 [11]. In spite of some contradiction these results confirmed on the whole again the existence of solar influence on the lower atmosphere. Different causal links are valid for either type of the relationships.

Within the scope of meteorological studies at this Symposium geomagnetic parameters have also been used for describing the solar activity (in this regard see also [12]). In our investigations we equally used days with strong geomagnetic storms as key days but this partial study did not result in new findings. Rather, the correlation becomes somewhat more complicated to define because the geomagnetic activity itself depends in a complex manner on the solar primary event (aside from a control by geomagnetic latitude, conditions of the inonosphere, and others).

Reference is also made to the publication of A.B. Pittock [13] because of its very accurate survey of literature. The given critical look deals mostly with long-term sun / weather relationships and their aspects regarding the global climate, nevertheless the short-term phenomena are discussed and positively assessed.

Within the scope of general meteorological considerations the latest study of Larsen and Kelly [14] should be mentioned because it deals also with the significance of weather forecasts. The authors state the following: "Approximately two days following a solar sector boundary crossing the accuracy of forecasting the positive vorticity assumes a minimum". This result is in some way related to our findings (see 3.6.) but we found that the predictive quality increases after boundary crossings and deteriorates before the sector crossing. This does not necessarily mean a contradiction because different kinds of meteorological forecasts have been used in both investigations.

The noted good correlation between the initial decrease of the galactic cosmic proton density before a flare and the subsequent Forbush effect on the one hand, and the immediately following variations of the total ozone and stratospheric intrusion frequency on the other, must be regarded as an essential part of our more recent results. We, therefore, refer at first to a series of publications dealing with the fundamental correlations between the sun and cosmic radiation, in particular with the Forbush decrease [15 - 21].
Neher and Anderson [15] have shown rather early the inverse correlation of both solar activity (sunspot number and geomagnetic activity) and the ion production in the stratosphere - though for very high northern geomagnetic latitude. This corresponds to the classical pattern of the long-term Forbush effect.

The work of [21] deals with a critical study of short-term phenomena in connection with Forbush-decreases where the relation to the individual parent flares between 1965 and 1976 has been analyzed.

The recurring sequence of decreasing neutron density, increasing total ozone, and subsequent triggering of stratospheric intrusions (see 3.5.) suggests to examine whether a physical link may possibly be invloved here.

It is a fact, that ionization and generation of exited nitrogen in the lower stratosphere are exclusively caused by the high energetic galactic cosmic rays. Only in very rare cases (after extremely vigorous flares) also solar protons reach the lower stratosphere for a period of minutes or some hours. These exceptional cases are so infrequent that they can be disregarded in the assessment of our statistically obtained results. On the other hand, the duration of the Forbush decrease is in the order of days.

Because the energy density loss of galactic cosmic rays is intensified in the lower stratosphere, the generation of ion pairs and exited nitrogen takes mainly place there (see e.g. [22 - 26]). The exited nitrogen atoms react with the oxygen molecules to form NO and O. Consequently, we find mainly in the lower stratosphere a dependence of the NO-concentration on the intensity of cosmic radiation (mainly galactic cosmic rays, rarely solar proton events) and thereby on the solar activity in general. Hence, an inverse correlation exists also between sunspot number and NO-concentration in the stratosphere following solar activity with a period of 11 years. According to [27] the estimated global, yearly production of NO varies between about 1.2×10^{33} at solar maximum and 1.8×10^{33} molecules at solar minimum. The amplitude of this variation increases however remarkably with growing geomagnetic magnitude so that the variation

in the NO-concentration in the stratosphere at latitudes $> 60^{o}$ should be essentially more pronounced which is suggested there also directly from the solar-related ion production. (Ion production and NO generation are directly proportional to each other [26]).Dickinson [24] points out that the greatest rate of ionization (and thus of NO production) happens near the tropopause.

Ruderman and Chamberlain [22] use the mentioned 11-year period of stratospheric NO-concentration for determining the expected periodicity and amplitude of the ozone concentration in the stratosphere. These considerations are based on the fact that part of the ozone is destroyed by NO. The authors find thus modulations of the stratospheric ozone concentration which are consistent with available measurements of time-lag, latitude dependence, and magnitude of cyclic variations of ozone. Whether these observations are quantitatively correct remains to be seen. (See in this regard the critical discussion in [28] which refers to an effect of fluctuating solar UV flux between 180 and 340 nm). Nevertheless it appears obvious to assume a direct correlation between the decrease of galactic cosmic rays and the increase of the total ozone. However, only one-dimensional models applying to long-term variations have been used so far in the calculation of chemical reactions and concentrations. Whether there may be also short-term reactions in the order of days remains undecided for the time being.

Mention be made here of the high ozone concentration observed by us in the lowest stratosphere after solar flares. The question of whether here the simultaneous decrease of the galactic cosmic ray density may be assumed as causative factor in terms of a physical link or whether another mechanism is involved must likewise be left open for the present time. We must also take into account that the high ozone in the lower stratosphere has been transported to our measuring station from

larger distances, mainly from northern latitudes. In fact, the Be7 collected during high peaks at our stations originates as a rule from latitudes $>60^{\circ}$. But just here, in the auroral belt, direct effects of galactic cosmic rays via chemical reactions are most likely to be expected.

Drastic variations in the ozone concentration in the lower stratosphere would next lead to temperature changes (via fluctuations of the stratospheric temperature profiles as a function of various trace gases)[29].
Stamnionis and Chamberlain [30] state:"The relationship between simple theory and observations is best at the lowest parts of the stratosphere, suggesting that the most direct control of ozone on temperature exists in the fairly inert region where ozone chemistry is umimportant and where the heating is due mainly to the absorption by ozone of direct solar ultraviolet and visual and terrestrial infrared radiation". Hence, a temperature change - in case of increasing ozone concentration above the tropopause a rise of temperature - might ultimately initiate a cyclogenesis and may, thereby, trigger the stratopsheric intrusions and alter the structure of the tropopause. These are first assumptions based on our most recent findings. Whether or not they are quantitatively realistic cannot be decided with certainty at this moment and even qualitative considerations remain unsolved for the present time.

Notwithstanding reference is made to the following observation of late [31]:"As the plasma (from the sun) is swept past the earth by its outward flow and the solar rotation, it impinges on the geomagnetosphere and deforms the magnetic cavity enclosing the earth. The main consequence of the interaction between the solar wind and the magnetosphere is the creation of magnetic field conditions that permit both entry and injection of high energy particles into the auroral latitudes on the earth. Such fluxes of particles alter

the ionization and temperature structure of the stratosphere at high latitude and may, thereby, influence circulation throughout our atmosphere."

Bassart and Yarger [32] observed, by the way, an influence of solar events on the height of the tropopause but these authors rely on dates of boundary crossings.

Finally, still one remark: It is no fundamental proof to the contrary that in a recent investigation [33] no correlation has been found between the atmospheric ozone profile and solar action induced by geomagnetic activity because this study is not based on daily profiles of the stratospheric ozone. But it is just that what our investigations have shown: Drastic fluctuations of the ozone in the stratosphere occur often from day to day and sometimes even in still shorter intervals of time. For significant results, daily ozone sonde flights are therefore a minimum demand.

Summing up, it must be said that the noted sequence: Forbush effect → temporary increase of the total ozone → sporadic peaks of ozone concentration in the lowermost stratosphere → and triggering of stratospheric intrusions is possibly due to a physical link. However, more in-depth studies are required over an extended period of time to confirm this conclusion.

References

[1] Reiter, R., Littfaß, M.: Stratospheric-Tropospheric Exchange Influenced by Solar Activity. Results of a 5-Year Study.
Arch.Met.Geoph.Biokl., Ser.A, 26, 127-154 (1977)

[2] Mahlman, J.D.: Relation of the Stratospheric-Tropospheric Mass Exchange Mechanism to Surface Radioactivity Peaks.
Arch.Met.Geoph.Biokl., Ser.A, 15, 1-25 (1965)

[3] Reiter, R.: Influences of Solar Activity on the Exchange Intensity Between Stratosphere and Troposphere.
McCormac, B.M., Proceedings: Solar Terrestrial Influences on Weather and Climate, Columbus, Ohio, 1978

[4] Müller, H., Reiter, R.: Intercomparison of New Zealand Filter and Dobson Photospectrometer for Total Ozone Measurement.
Prepared for Publication in PAGEOPH

[5] U.S. Department of Commerce. SOLAR GEOPHYISICAL DATA. Boulder, Colorado, 1969 - 1977.

[6] Bhatnagar, V.P. Jakobson, Th.: Lack of Effects of Solar Magnetic Sector Crossings on the Troposphere.
Geophys. Res. Letters, Vol.5, No.3, 180-182 (1978)

[7] Larsen, M.F.: Comment on the Paper "Lack of Effects Solar Magnetic Sector Crossings in the Troposphere" by Bhatnagar, V.P., Jakobson, T. (Paper 810440)
Geophys. Res. Letters, Vol.5, No.7, 619 (1978)

[8] Chamberlain, J.W.: A Mechanism for Inducing Climatic Variations Through the Stratosphere: Screening of Cosmic Rays by Solar and Terrestrial Magnetic Fields. J. Atmos. Sci., 34, 5, 737-743 (1977)

[9] Wilcox, J.M., Svalgaard, L., Scherrer, P.H.: On the Reality of a Sun-Weather Effect. J. Atmos. Sci., 33, 1113-1116 (1976)

[10] King, J.W.: Sun-Weather Relationships. Aeronautics and Astronautics, 13, 4, 10-19 (1975)

[11] Reiter, R.: Influences of Solar Activity on the Electric Potential Between the Ionosphere and the Earth.
McCormic, B.M., Proceedings: Solar-Terrestrial Influences on Weather and Climate, Columbus, Ohio, 1978

[12] Bucha, V.: Mechanism of Solar-Terrestrial Relations and Changes of the Atmospheric Circulation. Studia Geoph. et Geod., 21, 350-360 (1976)

[13] Pittock, A.B.: A Critical Look at Long-Term Sun-Weather Relationships. Rev. Geophys. Space Phys., 16, 400-420 (1978)

[14] Larsen, M.F., Kelley, M.C.: A Study of an Observed and Forecasted Meteorological Index and its Relation to the Interplanetary Magnetic Field. Geophys. Res. Letters, 4, 9 (1977)

[15] Neher, H.V., Anderson, H.R.: Cosmic Rays at Balloon Altitudes and the Solar Cycle. J. Geophys. Res., 67, 1309-1315 (1962)

[16] Neher, H.V.: Cosmic-Ray Particles that Changed from 1954 to 1958 to 1965. J. Geophys. Res., 72, 1527-1539 (1967)

[17] Lockwood, J.A.: Forbush Decrease in the Cosmic Radiation.
Space Science Reviews 12, 658-715 (1971)

[18] Daniel, R.R. Stephens, S.A.:Cosmic-Ray-Produced Electrons and Gamma Rays in the Atmosphere.
Rev. Geophys. Space Phys., 12 233-258 (1974)

[19] Pomerantz, M.A., Duggal, S.P.: The Sun and Cosmic Rays.
Rev. Geophys. Space Phys., 12, 343-362 (1974)

[20] Barouch, E., Burlaga, L.F.: Causes of Forbush Decreases and other Cosmic Ray Variations.
J. Geophys. Res., 80, 449-456 (1975)

[21] Křivský, L., Růžičková-Topolová, B.: Parameters of Forbush Decreases and their Parent Flares in the Solar Cycle 1965 - 1976.
Bull. Astron. Inst. Czechosl., 29, 30-44 (1978)

[22] Ruderman, M.A., Chamberlain, J.W.: Origin of the Sunspot Modulation of Ozone: Its Implications for Stratospheric NO Injection.
Planet. Space Sci., 23, 247-268 (1975)

[23] Warneck, P.: Cosmic Radiation as a Source of Odd Nitrogen in the Stratosphere.
J. Geophys. Res., 77, 6589-6591 (1972)

[24] Dickinson, R.E.: Solar Variability and the Lower Atmosphere.
Bull. Amer. Met. Soc., 56, 1240-1248 (1975)

[25] Crutzen, P.J., Isaksen, I., Reid, G.C.: Solar Proton Events: Stratospheric Sources of Nitric Oxide.
Science 189 , 457-459 (1975)

[26] Heaps, M.G.: Synopsis of Ionization Sources in the Mesosphere and Stratosphere, With Particular Emphasis given to the Path of the 25 February 1979 Solar Eclipse.
BRL Report No. 1938, October 1976

[27] World Meteorological Organization: Assessment of the Effect of Nitrogen Oxides on Ozone.
Final Report, September 1975

[28] Penner, J.E., Chang, J.S.: Possible Variations in Atmospheric Ozone Related to the Eleven Year Solar Cycle.
Geophys. Res. Letters, 5, 10, 817-820 (1978)

[29] Luther, F.M., Wuebbles, D.J., Chang, J.S.: Temperature Feedback in a Stratospheric Model.
J. Geophys. Res., 82, 4935-4942 (1977)

[30] Stanulonis, St.F., Chamberlain, J.W.: Thermal Response to Ozone Fluctuations of the Stratosphere.
J. Geophys. Res., 83, 6221-6223 (1978)

[31] White, O.R.: Solar Variability and Prediction.
In: Geophysical Predictions, 60-81, National Academy of Sciences, Washington D.C., 1978

[32] Basart, J.P., Yarger, D.N.:Preliminary Report of Changes in Tropopause Height Compared to Variations in Solar Behavior.
Private Communication (Internal Report)

[33] Weinbeck, R.S., Yarger, D,N.: Relationship of Atmospheric Ozone Profiles to Solar Magnetic Activity.
PAGEOPH 116 , 32-43 (1978)

VII. CONCLUSION

The works performed under contract on improved technical bases led in the reporting period to the following results:

Through lidar observations an aerosol layer can be detected in the lower stratosphere between 15 and 25 km altitude. The backscatter maximum is observed at an altitude of 17 to 22 km. The presently observed and rather low backscatter intensity is comparable to that noted before the eruption of volcano Fuego.

Based on 8-year recordings of the concentration of stratospheric radionuclides, ozone at 3 km altitude, and the total ozone, the influence of solar events on intrusions of stratopsheric air into the troposphere has been studied. Observed was a marked increase in the frequency of stratopsheric intrusions after H_α-flares and during Forbush effects. A significant, even though weak, influence of passages of the interplanetary magnetic field sector boundaries could likewise be established.

The causal relationships continue, however, to be unexplained. Consideration of all mechanisms that may come into question is needed to clarify this. Work hereon is in progress.

VIII. FUTURE PLANS

1. Continuation of aerosol sampling on the Zugspitze; determination of the concentration of cosmogenic radionuclides for detection of stratospheric intrusions into the biosphere.
2. Calculation of isentropic trajectories for long-term periods described in the present report; classification of tropospheric flow conditions relative to a climatology of stratospheric intrusions.

3. On the basis of a more extensive data material estimation of the mean stratospheric residence times by means of the activity ratio P32/Be7; re-checking of the earlier found seasonal differences.

4. Remote sensing of stratospheric aerosol layers up to 35 km altitude by means of lidar with simultaneous measurement of the aerological variables through radiosonde ascents of our own.

5. Application of the knowledge achieved as to the question of whether stratospheric intrusions influence the tropospheric ozone balance:

   a) Measurement of the ozone at 3 different levels in the lower troposphere,

   b) determination of the ozone balance with consideration of pollutants (e.g. NO_x, reactive hydrocarbons),

   c) effects of stratospheric intrusions on the tropospheric ozone.

6. Further studies of solar influences on stratospheric intrusions and on the structure of the stratospheric ozone profile.

ABSTRACT

The studies of the stratospheric-tropospheric exchange have been continued.

Continous data of the concentration of cosmogenic radionuclides Be7, P32, P33 as well as of fallout and daily means of ozone concentrations, measured at 3000 m ASL are presented for the reporting period.

Installation of two additional ozone measuring stations at 1800 and 740 m ASL provided the means for getting insight into the balance of the tropospheric ozone.

First results of routine monitoring of the stratospheric aerosol with a high resolution lidar are shown.
Accuracy of the method is discussed.

Control of the stratospheric-tropospheric exchange by solar activity is examined with the aid of the key day method using an 8-year measuring sequence. Relevant literature available on the subject is reviewed.

LEGENDS OF FIGURES

Fig. 1: Graphical representation of the concentration of fallout, Be7, P32, and ozone of the period August 1976 through October 1977

Fig. 2: Lidar backscattering profile and computed molecular return on 15 September 1977. Error bars denote one standard deviation of the photon counts.

Fig. 3: Analogous to Fig. 2; date 30 September 1977

Fig. 4: Ratios of measured total to calculated molecular backscattering. Horizontal bars (indicated by T on the left) denote the tropopause; solid line: Institute radiosonde; dashed line: Munich radiosonde. Period October 1976 through June 1977.

Fig. 5: Analogous to Fig. 4; period July 1977 - October 1977

Figs. 6 - 14 are uniformly plotted. They represent in all cases superposed epoch analyses around key days. The key days are indicated in each partial diagram by the sign ⏚. One and the same type of a key day, stated at bottom margin, applies to each one of the figures which all consist of several partial diagrams.

The vertically arranged partial diagram belong all to the same classification of data periods stated at the upper margin of the figure. The symbols following below stand for:

TOTAL: All data of the entire period from November 1969 through 1977;

SOLAR MAX: Period of maximum solar activity (e.g. data from November 1969 through 1972 inclusive);

SOLAR DECR: Period of decreasing solar activity (from 1973 through 1975);

SOLAR MIN: Period of solar quiet (e.g. data from January 1975 through February 1977).

The parameter being analyzed around the key day is stated on the left margin beside each line of the partial diagrams. The number of key days, taken as basis for each of the individual diagrams is indicated by N. The vertical bars represent the standard deviation. The superposed epoch analysis from -12 day before the key day to +12 day after the key day is plotted always from left to right.

Fig. 6 : Influence of season and polarity in the study of a correlation between Be7 and passage of a sector boundary as key day.

Fig. 7a: There is no influence of the phase of solar activity on the correlation Be7 $\leftrightarrow$ solar flares; however, the quotient P32:Be7 seems to depend on solar flares.

Fig. 7b: Correlation Be7 $\leftrightarrow$ H_α-flare, independent of the season.

Fig. 8 : Significant correlation of local ozone at 3 km altitude and total ozone with solar flares - except for minimum solar activity.

Fig. 9 : Solar flux and neutron density, showing a significant maximum around flare days independent of the phase of solar activity.

Fig. 10: Variation of the neutron density and solar flux around days with Forbush effect.

Fig. 11: Same as Fig.10 for geomagnetic index Ap and radio propagation index.

Fig. 12: Correlation between Be7 and quotient P32:Be7, respectively, and Forbush effect.

Fig. 13: Behavior of neutron density, total ozone, and local ozone at 3 km altitude around key days with maximum Be7 values.

Fig. 14: Conspicuous time sequence around H_α-flare key days (period of decreasing solar activity): 1. Beginning decrease of neutron density, 2. steep increase of the total ozone to reach a maximum, and 3. significant maximum of the Be7, 2 to 3 days after the key day.

FIGURES 1 - 14

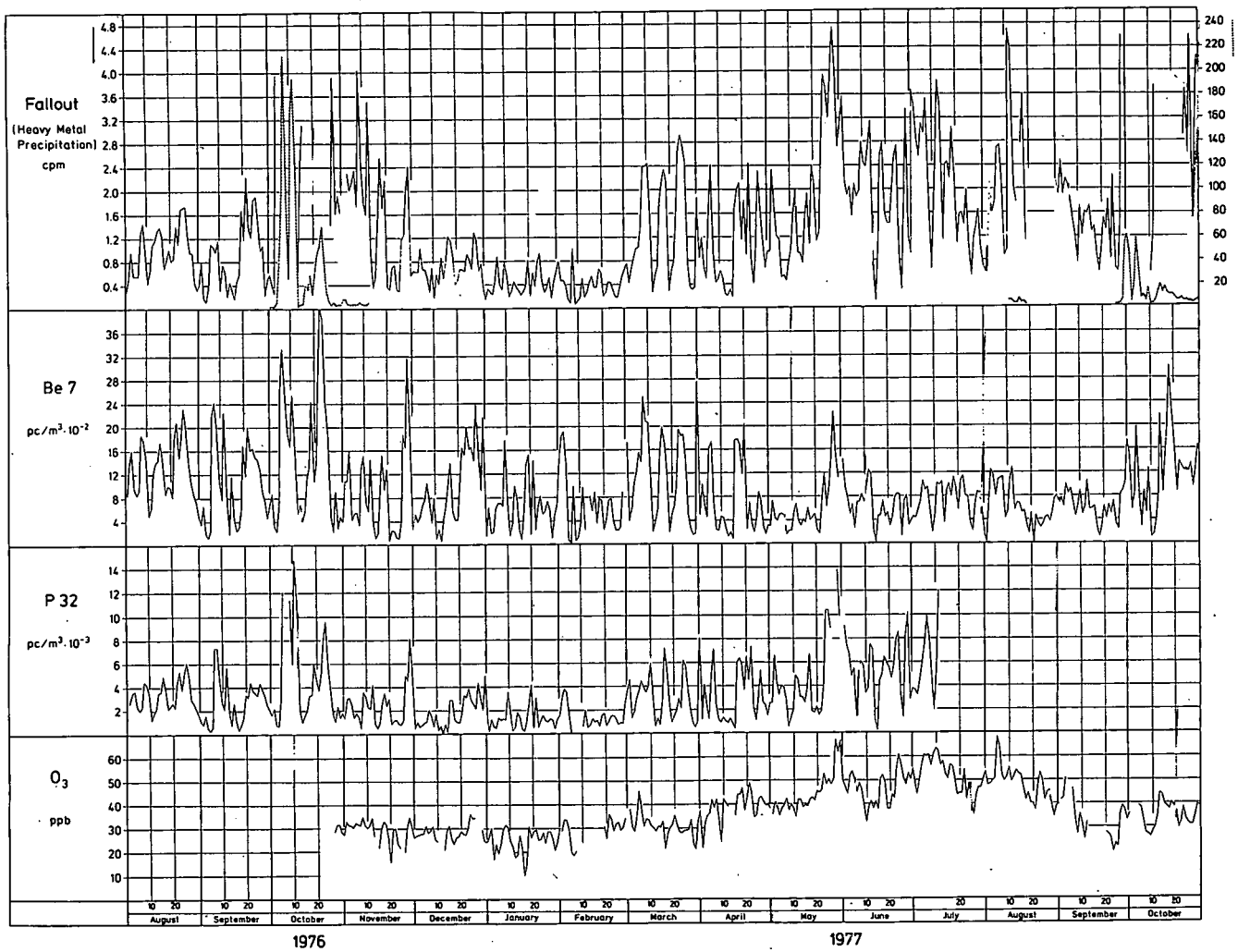
Fallout
(Heavy Metal Precipitation)
cpm
4.8
4.4
4.0
3.6
3.2
2.8
2.4
2.0
1.6
1.2
0.8
0.4
240
220
200
180
160
140
120
100
80
60
40
20
Be 7
pc/m³. 10⁻²
36
32
28
24
20
16
12
8
4
P 32
pc/m³. 10⁻³
14
12
10
8
6
4
2
O₃
ppb
60
50
40
30
20
10
10 20
August
September
October
November
December
January
February
March
April
May
June
July
August
September
October
1976
1977

Fig.1

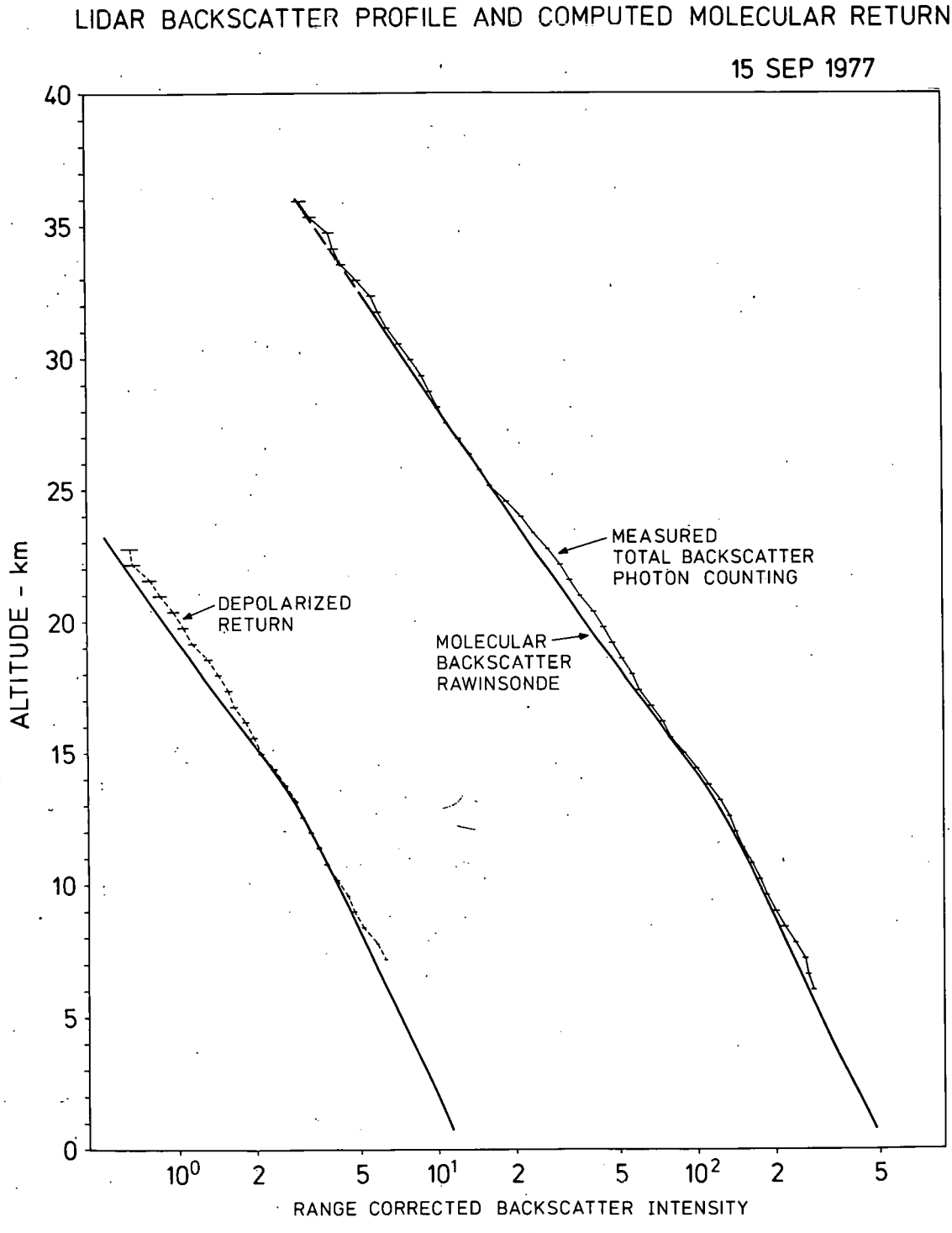
LIDAR BACKSCATTER PROFILE AND COMPUTED MOLECULAR RETURN
15 SEP 1977
ALTITUDE - km
40
35
30
25
20
15
10
5
0
DEPOLARIZED RETURN
MEASURED TOTAL BACKSCATTER PHOTON COUNTING
MOLECULAR BACKSCATTER RAWINSONDE
10^0
2
5
10^1
2
5
10^2
2
5
RANGE CORRECTED BACKSCATTER INTENSITY

Fig.2

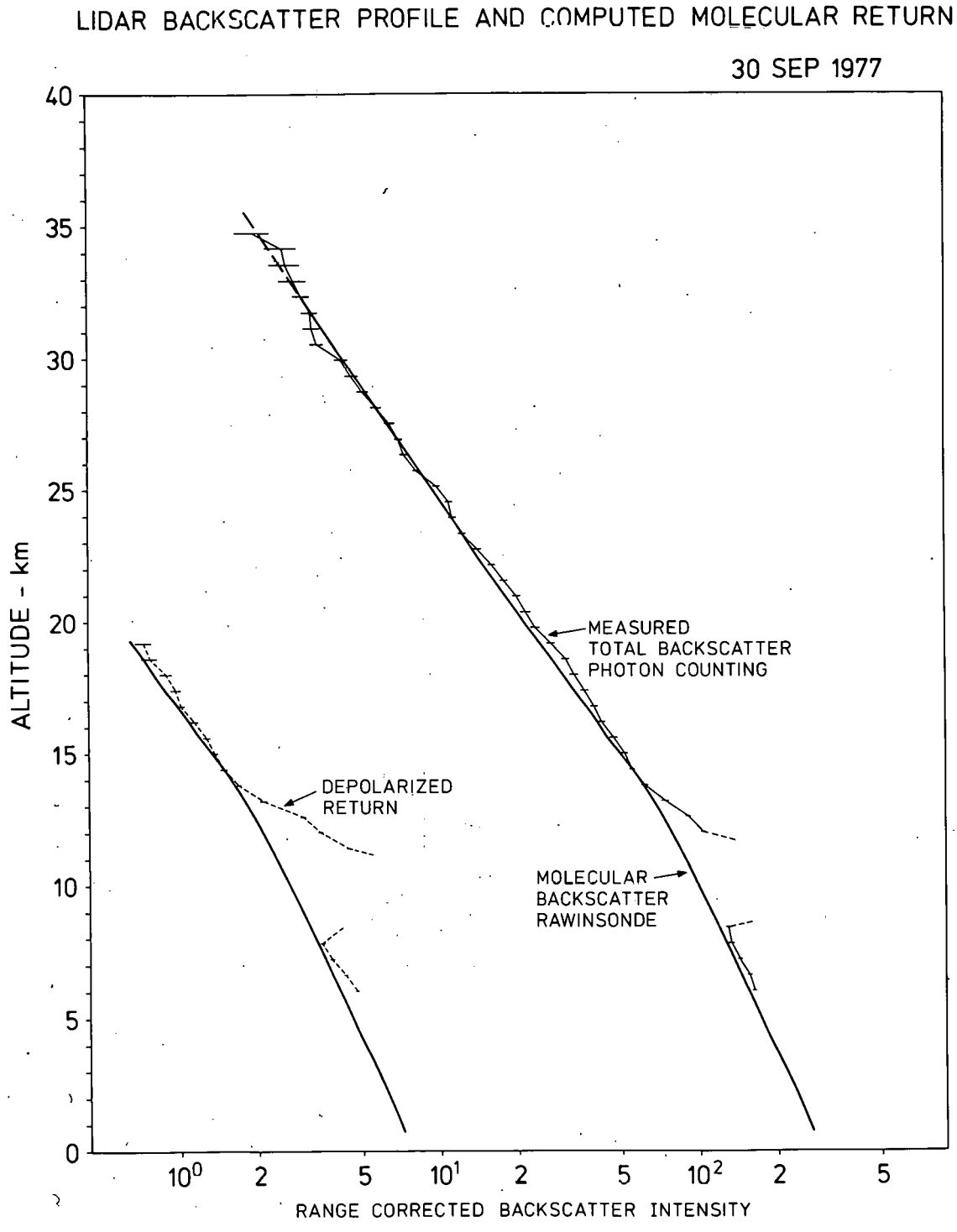
LIDAR BACKSCATTER PROFILE AND COMPUTED MOLECULAR RETURN
30 SEP 1977
ALTITUDE - km
40
35
30
25
20
15
10
5
0
MEASURED
TOTAL BACKSCATTER
PHOTON COUNTING
DEPOLARIZED
RETURN
MOLECULAR
BACKSCATTER
RAWINSONDE
10^0
2
5
10^1
2
5
10^2
2
5
RANGE CORRECTED BACKSCATTER INTENSITY

Fig.3

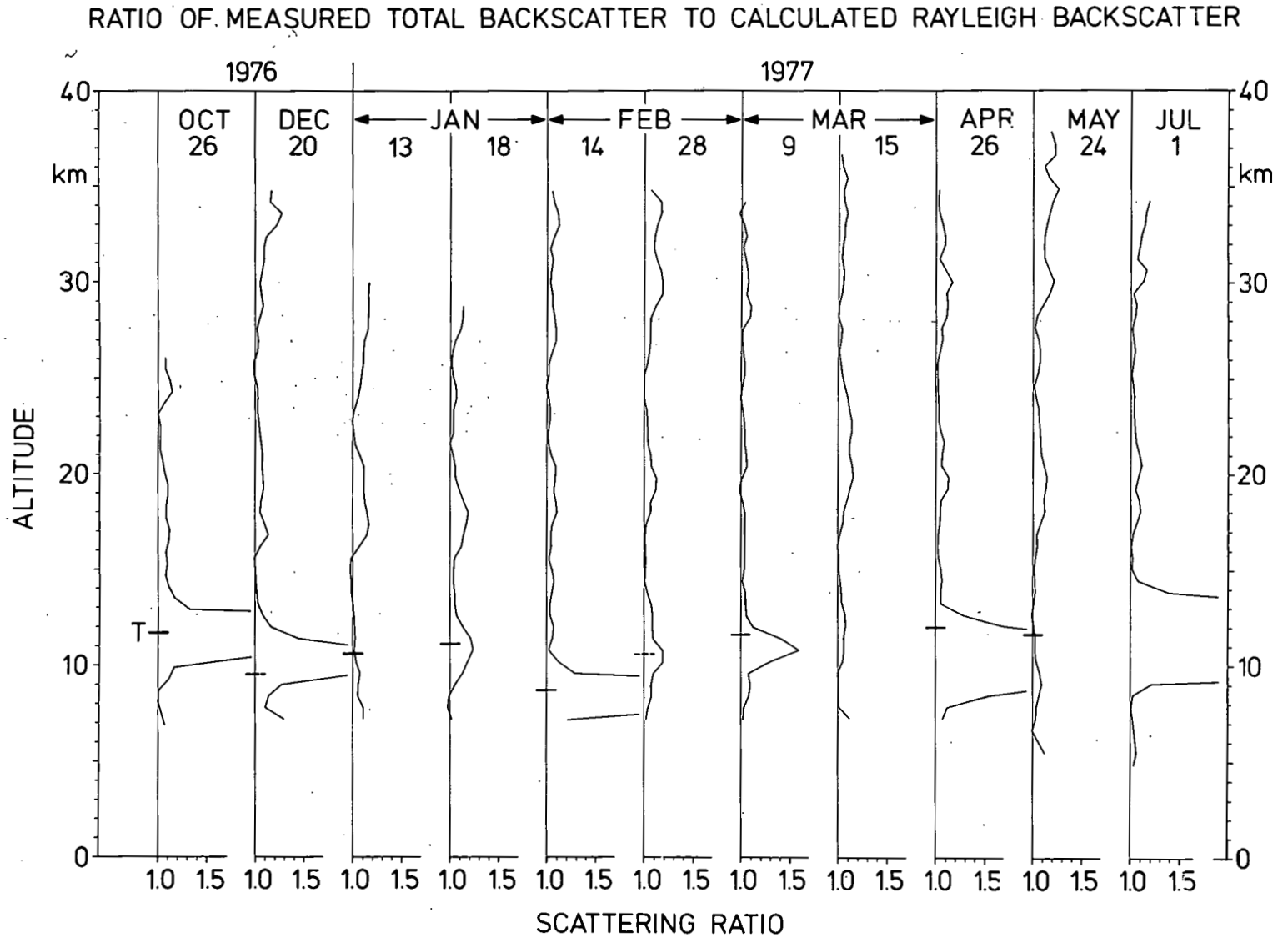
RATIO OF MEASURED TOTAL BACKSCATTER TO CALCULATED RAYLEIGH BACKSCATTER
1976
1977
OCT 26
DEC 20
JAN 13
JAN 18
FEB 14
FEB 28
MAR 9
MAR 15
APR 26
MAY 24
JUL 1
ALTITUDE
km
40
30
20
10
0
T
1.0 1.5
SCATTERING RATIO

Fig. 4

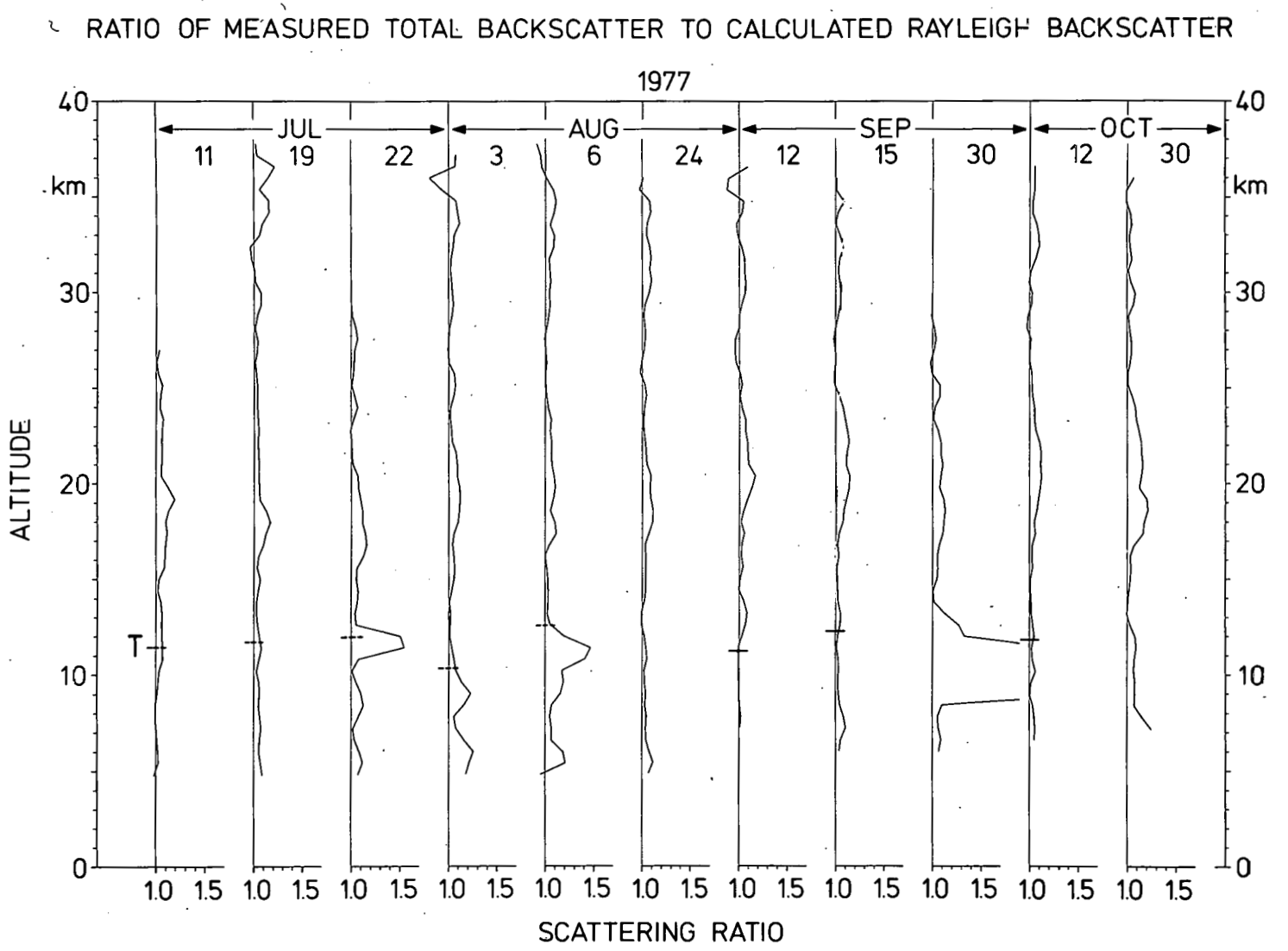
RATIO OF MEASURED TOTAL BACKSCATTER TO CALCULATED RAYLEIGH BACKSCATTER
1977
JUL
AUG
SEP
OCT
11
19
22
3
6
24
12
15
30
12
30
ALTITUDE
km
40
30
20
10
0
T
1.0
1.5
SCATTERING RATIO

Fig. 5

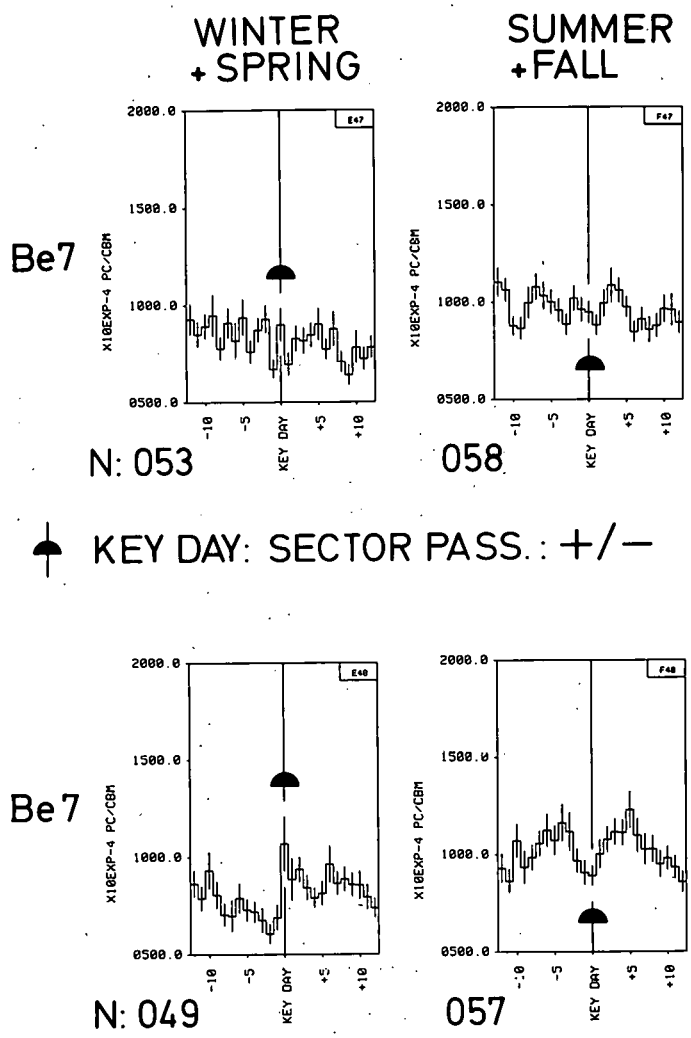
WINTER
+SPRING
SUMMER
+FALL
Be7
2000.0
1500.0
1000.0
0500.0
X10EXP-4 PC/CBM
E47
F47
-10
-5
KEY DAY
+5
+10
N: 053
058
KEY DAY: SECTOR PASS.: +/−
E48
F48
N: 049
057
KEY DAY: SECTOR PASS.: −/+

Fig.6

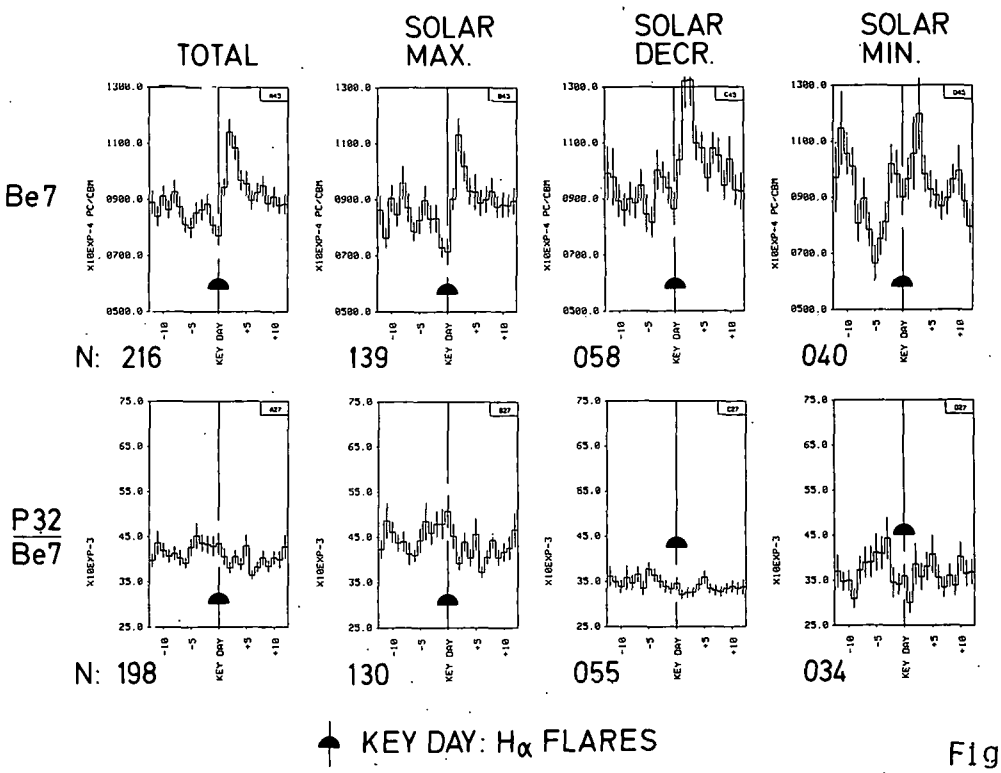
TOTAL
SOLAR MAX.
SOLAR DECR.
SOLAR MIN.
Be7
P32/Be7
N: 216
139
058
040
N: 198
130
055
034
KEY DAY: Hα FLARES

Fig.7a

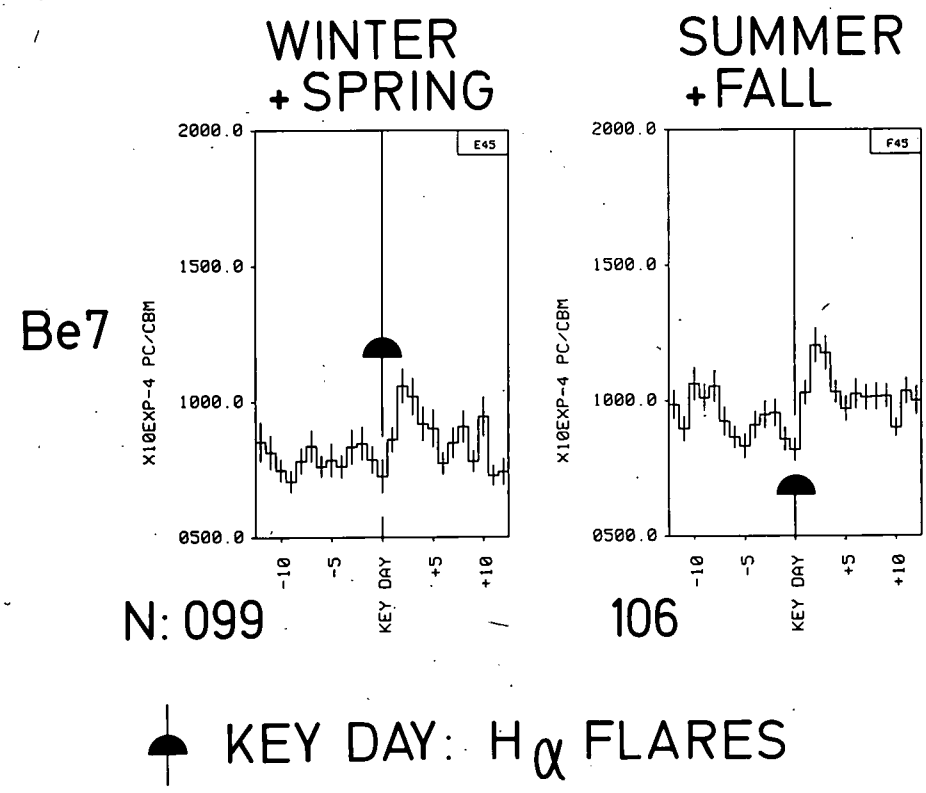

KEY DAY: $H\alpha$ FLARES

Fig.7b

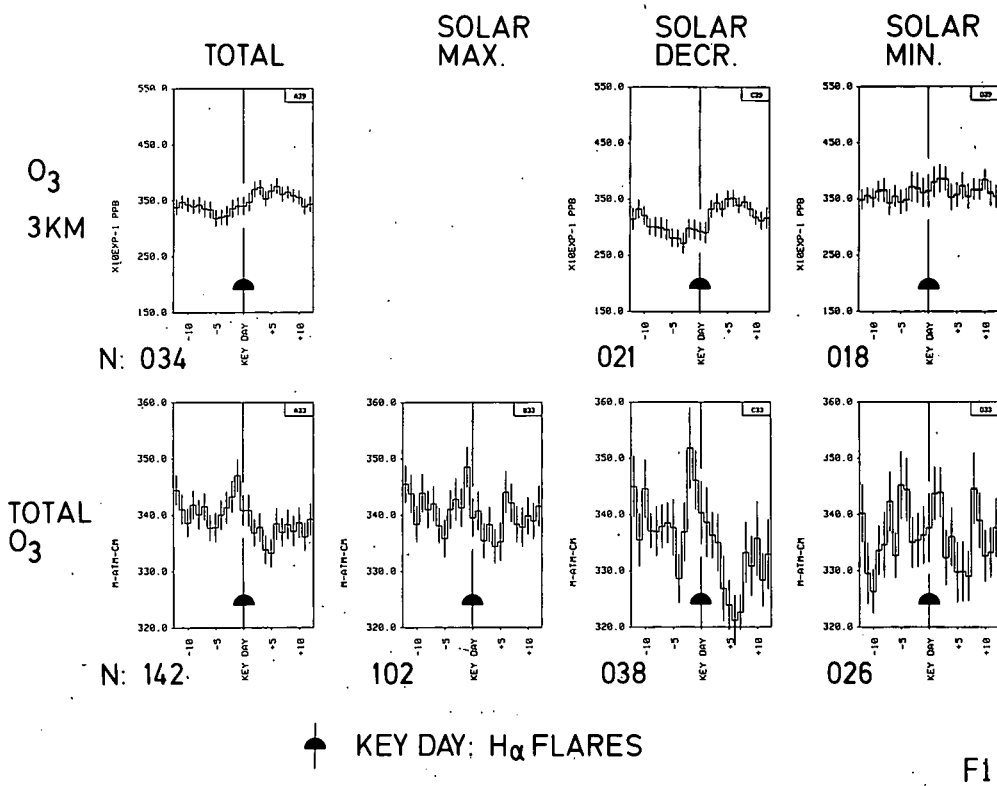
TOTAL
SOLAR MAX.
SOLAR DECR.
SOLAR MIN.
O_3 3KM
X10EXP-1 PPB
N: 034
021
018
TOTAL O_3
M-ATM-CM
N: 142
102
038
026
KEY DAY
KEY DAY: Hα FLARES

Fig.8

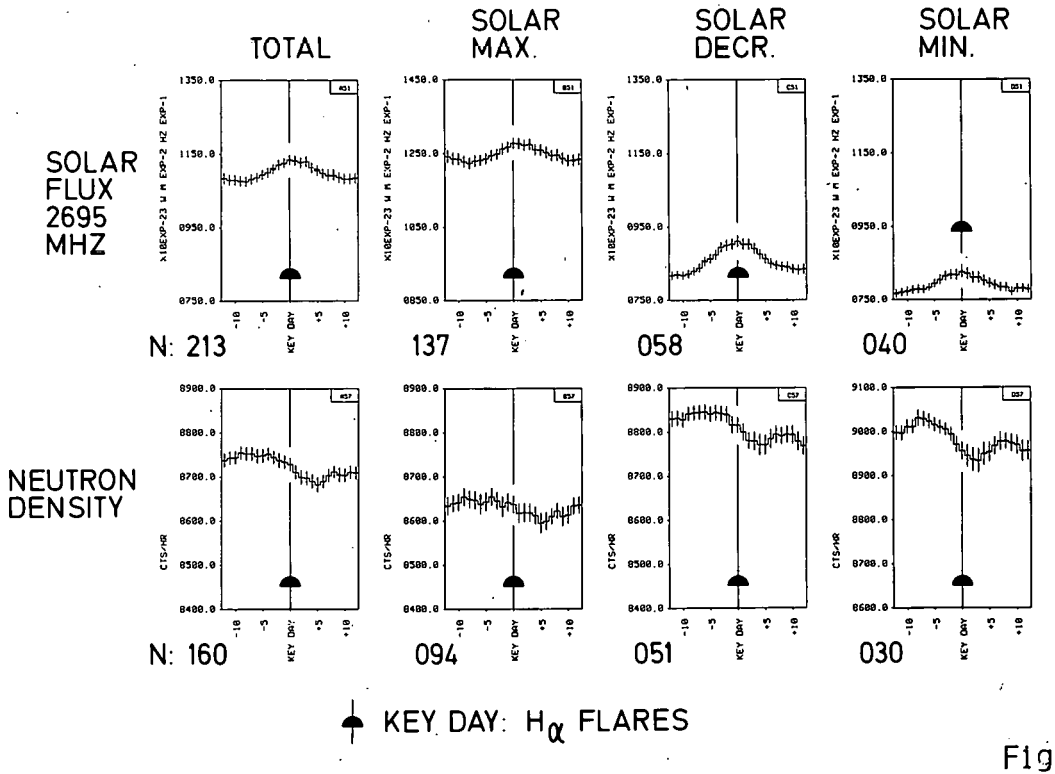
TOTAL
SOLAR MAX.
SOLAR DECR.
SOLAR MIN.
SOLAR FLUX 2695 MHZ
NEUTRON DENSITY
N: 213
137
058
040
N: 160
094
051
030
KEY DAY: Hα FLARES

Fig.9

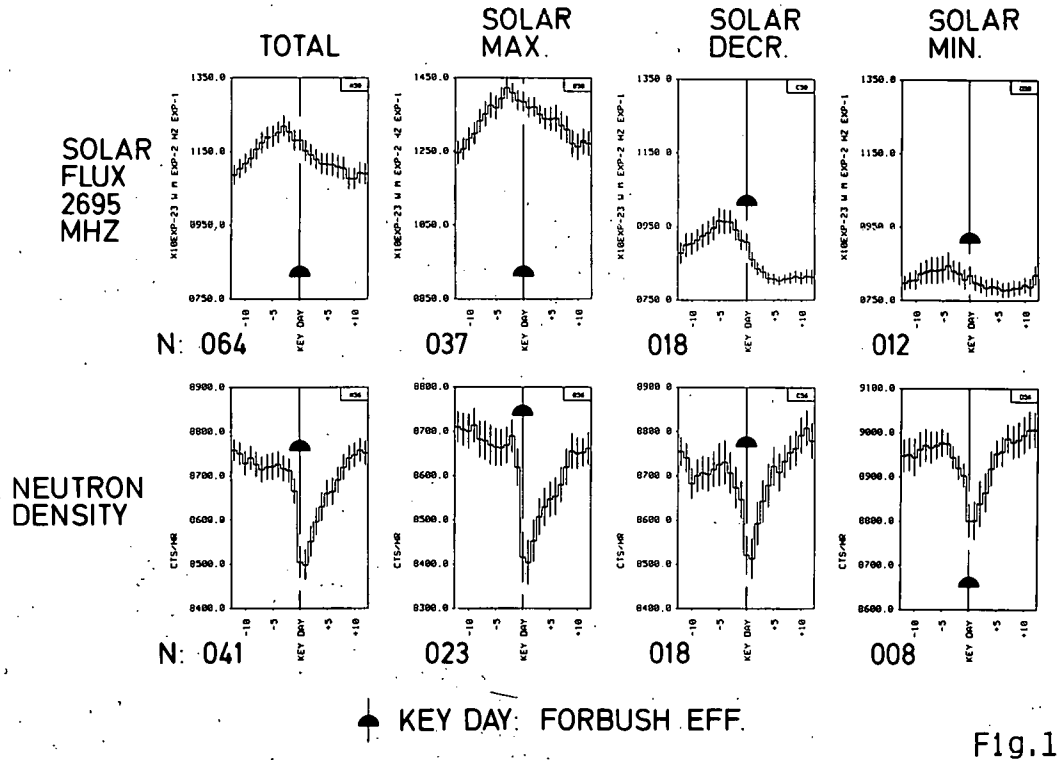
TOTAL
SOLAR MAX.
SOLAR DECR.
SOLAR MIN.
SOLAR FLUX 2695 MHZ
N: 064
037
018
012
NEUTRON DENSITY
N: 041
023
018
008
KEY DAY: FORBUSH EFF.

Fig.10

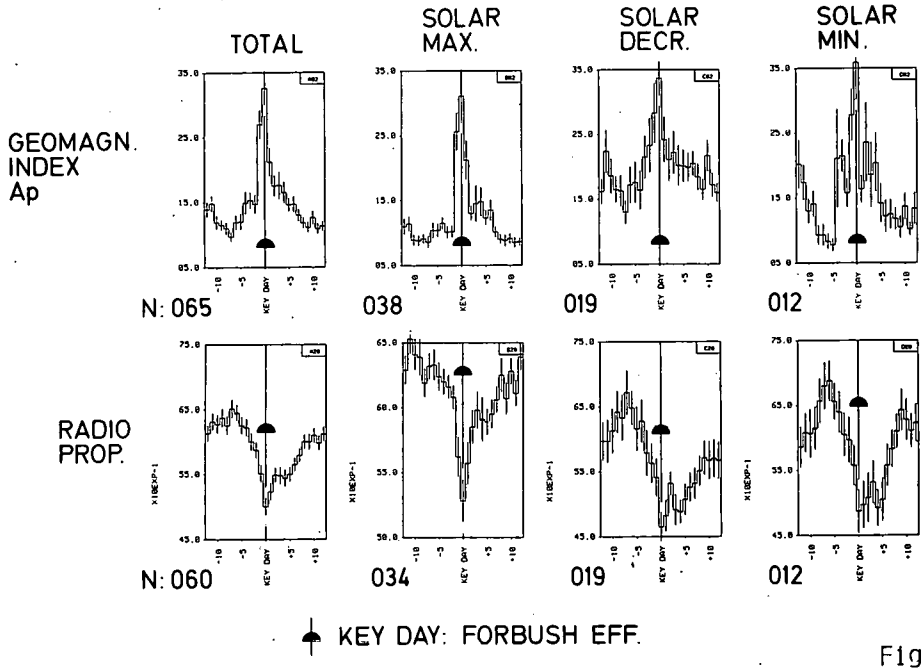
TOTAL
SOLAR MAX.
SOLAR DECR.
SOLAR MIN.
GEOMAGN. INDEX Ap
N: 065
038
019
012
RADIO PROP.
N: 060
034
019
012
KEY DAY
KEY DAY: FORBUSH EFF.

Fig.11

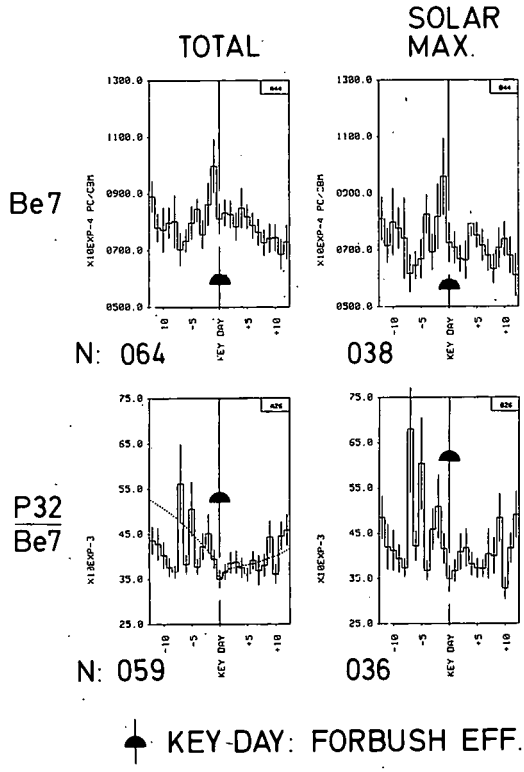
TOTAL
SOLAR MAX.
Be7
P32/Be7
N: 064
038
N: 059
036
KEY DAY
KEY-DAY: FORBUSH EFF.

Fig.12

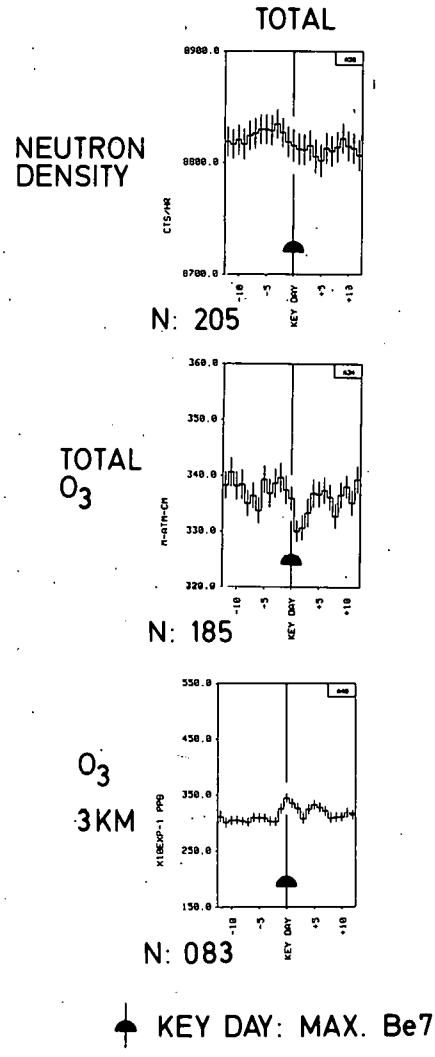
TOTAL
NEUTRON DENSITY
8900.0
8800.0
8700.0
CTS/HR
-10
-5
KEY DAY
+5
+10
N: 205
TOTAL O_3
360.0
350.0
340.0
330.0
320.0
n-ATM-CM
N: 185
O_3 3KM
550.0
450.0
350.0
250.0
150.0
X10E2P-1 PPB
N: 083
KEY DAY: MAX. Be7

Fig. 13

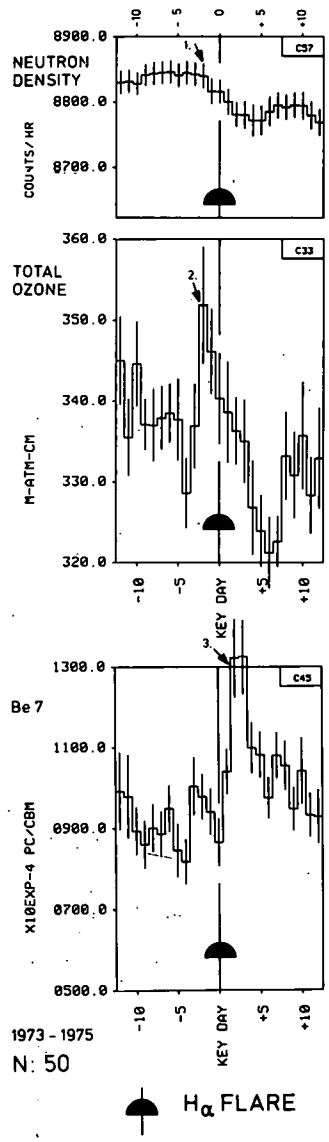
-10
-5
0
+5
+10
8900.0
NEUTRON DENSITY
8800.0
COUNTS/HR
8700.0
C37
1.
360.0
TOTAL OZONE
350.0
340.0
M-ATM-CM
330.0
320.0
C33
2.
-10
-5
KEY DAY
+5
+10
3.
1300.0
Be 7
1100.0
X10EXP-4 PC/CBM
0900.0
0700.0
0500.0
C45
-10
-5
KEY DAY
+5
+10
1973 - 1975
N: 50
Hα FLARE

Fig.14

A N N E X

Results of Diurnal Measurements

T A B L E S I - XV

Diurnal concentrations of Be7, P32, P33, and some fallout elements (heavy metals) in the air at 2964 m a.s.l.
(Zugspitze peak)

Radioactivity pc/m^3

Aug 1976	fallout $.10^{-2}$	Be7 $.10^{-2}$	P32 $.10^{-3}$	P33 $.10^{-3}$	O_3 ppb
1	0.27	8.49	2.59	1.84	*/.
2	0.49	13.47	3.49	2.92	*/.
3	0.94	16.03	3.66	3.27	*/.
4	0.53	9.47	2.35	1.94	*/.
5	0.53	8.43	1.97	2.12	*/.
6	0.53	9.32	2.32	2.25	*/.
7	1.23	18.66	4.47	4.24	*/.
8	1.43	17.75	4.21	3.66	*/.
9	0.94	15.04	3.56	3.23	*/.
10	0.40	4.91	1.16	1.04	*/.
11	0.61	6.26	1.77	1.43	*/.
12	1.06	12.04	2.18	2.42	*/.
13	1.13	13.88	3.49	2.50	*/.
14	1.29	14.37	3.58	3.36	*/.
15	1.37	17.44	4.94	3.32	*/.
16	1.22	14.09	3.85	4.12	*/.
17	0.66	8.59	2.14	1.95	*/.
18	0.80	10.04	2.38	1.92	*/.
19	0.98	9.73	2.66	2.65	*/.
20	0.78	8.04	2.21	2.25	*/.
21	0.82	17.93	4.36	3.91	*/.
22	1.38	20.89	5.32	4.47	*/.
23	1.07	14.80	3.72	3.02	*/.
24	1.67	18.14	5.07	4.40	*/.
25	1.70	23.20	6.09	3.56	*/.
26	1.72	19.67	4.99	3.00	./.
27	1.22	13.96	2.92	1.42	./.
28	0.93	10.31	2.60	1.52	*/.
29	0.92	8.45	2.13	0.90	./.
30	0.41	7.23	1.62	0.88	*/.
31	0.29	4.80	1.06	0.79	*/.

Radioactivity pc/m^3

Sep 1976	fallout $.10^{-2}$	Be7 $.10^{-2}$	P32 $.10^{-3}$	P33 $.10^{-3}$	O_3 ppb
1	0.39	3.43	0.78	0.58	*/.
2	0.75	6.60	1.56	1.31	*/.
3	0.16	1.89	0.50	0.58	*/.
4	0.09	1.13	0.26	0.30	*/.
5	0.33	2.39	0.58	0.48	*/.
6	1.08	21.66	7.30	3.15	*/.
7	1.03	24.25	7.34	3.29	*/.
8	0.93	19.83	4.70	4.41	*/.
9	1.13	10.74	2.68	2.27	*/.
10	0.28	7.63	2.05	0.66	*/.
11	0.72	22.49	5.69	4.12	*/.
12	0.59	8.37	1.94	0.94	*/.
13	0.18	1.77	0.71	0.90	*/.
14	0.43	11.55	2.63	1.41	*/.
15	0.29	4.52	1.12	0.83	*/.
16	0.14	2.30	0.31	0.43	*/.
17	0.43	2.95	0.73	0.61	*/.
18	0.55	6.01	1.34	0.57	*/.
19	1.66	16.87	3.34	2.34	*/.
20	1.15	11.65	3.07	2.07	*/.
21	2.22	20.05	4.39	3.10	*/.
22	1.36	15.97	3.71	2.38	*/.
23	1.19	16.39	3.47	2.50	*/.
24	1.83	14.92	3.26	1.79	*/.
25	1.89	14.50	4.32	3.38	*/.
26	1.43	12.91	3.76	2.75	*/.
27	0.96	9.30	3.28	2.16	*/.
28	1.05	7.45	2.49	1.58	*/.
29	0.20	4.52	2.07	0.93	*/.
30	0.46	6.56	1.60	1.78	*/.

III

Radioactivity pc/m^3

Oct 1976	fallout $.10^{-2}$	Be7 $.10^{-2}$	P32 $.10^{-3}$	P33 $.10^{-3}$	O_3 ppb
1	0.55	8.54	2.16	1.87	*/.
2	0.38	3.03	0.77	1.13	*/.
3	0.23	2.14	0.62	1.25	*/.
4	3.93	6.46	2.83	1.92	*/.
5	37.61	26.90	12.04	12.46	*/.
6	93.74	33.20	17.07	20.53	*/.
7	212.76	25.64	19.12	31.92	*/.
8	93.03	18.92	11.38	17.69	*/.
9	23.84	16.64	5.89	6.12	*/.
10	160.39	25.42	14.73	29.91	*/.
11	193.37	16.84	11.36	21.54	*/.
12	111.82	5.23	1.96	2.57	*/.
13	0.61	6.82	0.95	0.86	*/.
14	2.34	3.97	1.54	1.83	*/.
15	3.09	5.80	1.99	2.49	*/.
16	17.99	11.18	3.25	4.24	*/.
17	15.14	13.33	3.29	5.41	*/.
18	27.44	24.30	5.91	12.15	*/.
19	10.00	10.65	4.60	4.90	*/.
20	29.45	13.99	3.65	8.43	*/.
21	45.27	28.00	5.07	17.13	*/.
22	51.67	40.47	8.01	21.04	*/.
23	68.37	38.27	9.57	28.83	*/.
24	38.73	24.36	5.69	18.44	*/.
25	12.51	18.83	3.71	8.37	*/.
26	5.04	4.90	1.65	3.62	*/.
27	1.40	2.08	0.99	0.99	28.22
28	3.90	8.98	2.32	3.58	31.23
29	1.59	2.70	1.33	1.76	31.42
30	1.90	4.73	1.75	3.32	28.26
31	1.61	3.82	1.29	2.33	27.00

Radioactivity pc/m^3

Nov 1976	fallout $.10^{-2}$	Be7 $.10^{-2}$	P32 $.10^{-3}$	P33 $.10^{-3}$	O_3 ppb
1	6.42	10.58	2.95	6.46	32.68
2	6.37	10.78	3.06	6.44	31.17
3	2.28	15.80	2.49	3.06	31.04
4	1.99	4.10	1.32	1.22	30.07
5	2.12	5.18	1.74	2.29	32.10
6	2.33	5.41	1.42	2.12	31.62
7	1.72	3.22	0.41	0.73	31.00
8	4.02	12.73	3.56	6.54	34.91
9	2.38	15.01	3.14	3.80	31.01
10	1.79	6.96	2.22	3.67	29.93
11	1.57	5.56	2.09	2.73	31.17
12	3.49	14.40	4.16	6.81	34.36
13	0.99	3.71	0.84	1.25	26.45
14	0.32	0.94	0.43	0.67	*/.
15	0.51	1.78	0.89	0.68	21.49
16	1.51	8.56	2.51	3.53	29.48
17	2.54	15.14	3.45	4.95	32.83
18	1.69	9.17	2.32	3.93	31.55
19	2.16	12.72	2.95	4.90	25.99
20	0.34	0.55	0.77	0.99	15.27
21	0.29	2.28	1.08	1.07	29.03
22	0.66	2.19	1.16	0.97	29.84
23	0.71	1.11	0.82	0.32	23.24
24	0.29	0.92	0.75	0.48	21.55
25	0.26	3.72	1.10	0.61	*/.
26	1.15	18.55	4.92	4.64	19.74
27	1.22	16.37	4.45	4.76	29.88
28	1.99	31.51	8.10	9.72	34.58
29	2.39	19.91	4.84	6.17	30.59
30	0.53	2.55	0.40	0.43	25.88

Radioactivity pc/m^3

Dec 1976	fallout $.10^{-2}$	Be7 $.10^{-2}$	P32 $.10^{-3}$	P33 $.10^{-3}$	O_3 ppb
1	0.61	4.99	0.94	1.53	26.70
2	0.59	3.70	0.53	2.44	27.01
3	0.59	4.58	0.70	1.82	27.46
4	1.00	6.35	0.87	2.14	27.67
5	0.64	7.44	1.02	1.88	30.95
6	0.63	10.33	2.01	2.13	27.80
7	0.50	7.37	1.47	2.30	28.89
8	0.25	3.59	0.56	0.93	30.86
9	0.67	7.78	1.65	2.27	25.11
10	0.15	0.87	0.24	0.84	24.19
11	0.55	2.47	0.63	1.13	*/.
12	0.38	0.41	0.01	0.36	*/.
13	0.84	4.12	0.79	1.82	20.70
14	0.48	6.40	0.11	2.02	28.73
15	0.77	9.95	2.81	2.67	30.99
16	1.20	13.71	2.81	2.98	25.47
17	1.12	5.35	1.11	0.99	22.97
18	0.86	4.02	0.97	1.24	25.92
19	0.38	3.99	0.89	1.06	26.32
20	0.45	10.33	1.65	2.06	28.60
21	0.64	16.37	3.21	4.12	27.38
22	0.63	15.03	3.03	3.49	26.99
23	0.60	19.72	3.82	3.34	29.77
24	0.90	16.05	2.78	2.67	35.90
25	0.80	16.41	2.47	2.99	33.98
26	0.64	14.03	2.06	2.62	34.21
27	1.27	23.58	4.31	5.43	*/.
28	1.14	15.52	3.01	3.30	*/.
29	0.61	9.04	1.95	2.46	29.27
30	0.73	21.50	4.91	4.24	24.35
31	0.28	4.75	1.17	1.64	23.92

Radioactivity pc/m^3

Jan 1977	fallout $.10^{-2}$	Be7 $.10^{-2}$	P32 $.10^{-3}$	P33 $.10^{-3}$	O_3 ppb
1	0.14	1.37	0.16	0.65	26.22
2	0.32	6.17	1.17	1.70	30.07
3	0.26	1.83	0.56	0.47	16.59
4	0.22	2.01	0.44	0.53	23.18
5	0.45	6.01	1.31	2.49	19.09
6	0.87	6.89	1.11	1.98	23.11
7	0.39	6.96	1.22	2.59	29.35
8	0.30	6.38	1.15	1.90	31.26
9	0.76	17.70	3.51	4.60	30.32
10	0.54	7.00	1.77	2.34	24.49
11	0.18	1.33	0.19	1.20	22.18
12	0.28	3.41	0.48	1.25	17.39
13	0.44	9.84	1.78	2.37	18.53
14	0.34	7.64	1.36	2.14	26.90
15	0.29	2.36	0.38	0.95	21.28
16	0.21	0.74	0.15	0.47	9.71
17	0.27	5.35	1.04	1.45	15.07
18	0.36	13.33	2.50	3.08	30.64
19	0.81	15.18	4.14	4.45	25.81
20	0.20	1.60	0.46	0.80	28.59
21	0.59	14.19	3.03	4.25	29.25
22	0.36	2.36	0.48	1.22	24.83
23	0.76	6.16	1.07	2.67	25.25
24	0.93	8.16	1.52	2.27	28.10
25	0.44	5.06	1.08	1.87	23.49
26	0.26	5.58	0.97	2.26	28.48
27	0.34	7.24	1.22	1.83	28.50
28	0.51	5.76	1.14	1.11	25.43
29	0.16	0.94	0.35	0.38	20.33
30	0.44	4.75	1.15	1.51	23.96
31	0.61	6.54	1.47	1.52	29.49

Radioactivity pc/m^3

Feb 1977	falloul $.10^{-2}$	De7 $.10^{-2}$	P32 $.10^{-3}$	P33 $.10^{-3}$	O_3 ppb
1	0.78	13.63	2.86	3.13	28.66
2	0.45	18.20	3.74	4.68	33.50
3	0.46	19.08	3.49	7.07	33.17
4	0.37	13.78	1.75	4.61	29.22
5	0.14	0.62	0.08	0.65	19.57
6	0.07	0.13	--	0.47	18.21
7	1.00	9.76	1.85	4.41	19.94
8	0.05	0.50	*/.	0.40	*/.
9	0.11	1.08	--	0.59	*/.
10	0.16	3.33	0.56	1.97	*/.
11	0.49	9.59	1.90	4.94	*/.
12	0.17	2.35	0.46	1.58	*/.
13	0.26	*/.	0.65	2.13	*/.
14	0.42	7.97	1.21	3.22	*/.
15	0.53	5.53	0.92	2.41	*/.
16	0.34	8.79	1.07	2.61	*/.
17	0.34	3.46	0.53	2.03	*/.
18	0.65	7.61	1.46	4.32	*/.
19	0.58	7.29	1.68	4.50	30.51
20	0.19	2.36	0.60	2.09	25.25
21	0.25	4.14	0.99	2.75	35.92
22	0.43	7.30	1.43	4.36	33.88
23	0.42	7.59	1.45	4.31	28.69
24	0.30	3.94	1.22	1.03	31.72
25	0.18	2.34	0.70	0.46	32.55
26	0.17	2.25	0.86	1.46	29.01
27	0.34	2.77	0.80	0.85	30.24
28	0.53	8.75	2.60	1.98	34.12

Radioactivity pc/m^3

March 1977	fallout $.10^{-2}$	Be7 $.10^{-2}$	P32 $.10^{-3}$	P33 $.10^{-3}$	O_3 ppb
1	0.74	17.22	4.51	3.50	37.92
2	0.41	3.87	1.26	1.55	30.59
3	0.65	6.01	1.81	2.64	28.43
4	0.83	10.00	2.91	3.69	35.23
5	0.99	12.00	3.52	4.16	45.79
6	1.01	15.49	4.42	5.40	37.53
7	1.36	13.84	3.88	7.74	30.56
8	2.39	25.02	3.42	8.25	33.82
9	2.39	20.82	3.94	8.99	33.38
10	2.44	20.62	5.91	8.96	30.86
11	1.60	11.31	3.16	4.41	30.18
12	0.25	1.98	0.54	0.96	28.58
13	0.53	3.92	1.26	1.98	30.64
14	0.67	5.86	0.68	6.52	30.27
15	1.77	15.68	2.72	9.65	32.94
16	2.10	19.77	7.22	19.55	21.02
17	2.34	17.02	5.38	15.62	27.23
18	2.12	11.98	2.53	11.92	30.07
19	0.27	1.91	0.86	10.23	31.44
20	0.61	4.94	1.44	8.61	35.34
21	0.76	6.29	1.87	10.63	31.25
22	1.56	9.86	2.92	13.67	28.27
23	2.64	19.41	2.07	7.83	27.75
24	2.92	18.31	6.16	23.89	28.74
25	2.73	18.51	5.67	19.75	29.03
26	2.48	14.29	3.61	14.98	29.22
27	0.74	4.82	1.97	10.11	33.71
28	0.34	2.57	0.90	11.57	23.38
29	0.30	1.44	0.45	7.90	20.84
30	0.34	1.63	0.91	7.07	32.57
31	1.86	27.49	8.05	18.70	37.29

IX

Radioactivity pc/m^3

Apr 1977	fallout $.10^{-2}$	Be7 $.10^{-2}$	P32 $.10^{-3}$	P33 $.10^{-3}$	O_3 ppb
1	0.84	4.84	1.13	8.39	21.31
2	1.18	10.04	1.09	15.66	31.85
3	0.68	6.61	2.35	10.25	35.16
4	0.48	4.44	1.17	5.77	35.98
5	1.54	16.17	4.85	11.84	42.02
6	2.42	17.31	7.14	28.59	38.45
7	0.88	6.47	2.41	14.82	42.15
8	0.41	2.29	1.14	10.92	33.15
9	0.48	2.16	0.86	9.00	23.83
10	0.62	4.54	1.28	8.62	42.36
11	0.48	4.36	1.02	7.53	40.43
12	0.22	2.48	0.82	7.11	39.09
13	0.19	1.12	1.23	1.54	*/.
14	0.30	1.93	0.80	11.37	*/.
15	0.17	0.66	0.35	9.39	35.08
16	1.69	17.49	5.95	16.24	44.05
17	1.98	17.74	6.34	15.60	44.07
18	2.11	16.79	5.80	15.34	46.96
19	1.14	11.67	3.61	11.53	37.18
20	1.81	20.37	6.48	18.01	42.64
21	0.88	2.34	4.42	15.35	49.02
22	2.44	6.92	7.36	21.87	44.68
23	0.83	3.40	2.13	9.82	34.34
24	0.39	1.80	1.04	7.08	35.29
25	1.01	4.06	2.76	12.21	41.95
26	2.31	8.67	5.29	13.44	43.27
27	1.67	7.05	2.58	3.98	41.33
28	1.12	2.79	2.35	13.09	39.50
29	0.66	1.47	1.43	8.97	39.75
30	0.94	2.95	2.51	8.73	38.18

Radioactivity pc/m^3

May 1977	fallout $.10^{-2}$	Be7 $.10^{-2}$	P32 $.10^{-3}$	P33 $.10^{-3}$	O_3 ppb
1	0.94	2.95	2.51	8.73	35.66
2	2.33	7.15	6.57	20.44	40.87
3	1.69	4.25	4.22	13.79	39.01
4	1.20	3.73	3.10	16.26	35.01
5	1.15	4.88	3.99	18.91	38.35
6	0.50	4.96	3.80	11.73	39.61
7	0.54	4.67	2.80	9.33	42.51
8	0.44	1.42	0.48	4.99	37.26
9	0.76	2.09	1.24	3.45	40.08
10	0.97	2.02	1.86	10.60	38.04
11	1.57	4.86	4.87	16.08	34.46
12	1.97	6.66	4.53	18.94	42.06
13	0.92	3.83	3.00	13.40	41.82
14	0.91	2.90	3.01	11.43	38.68
15	0.74	4.00	2.52	11.69	39.60
16	1.47	3.46	3.76	9.68	38.99
17	1.93	5.94	6.65	16.21	42.03
18	1.06	3.89	1.85	2.57	42.89
19	2.40	4.39	1.67	1.80	41.45
20	2.10	4.96	2.25	2.91	45.57
21	1.11	2.28	1.47	2.13	44.80
22	1.26	1.56	1.84	4.16	46.00
23	2.63	7.04	4.03	9.62	52.95
24	3.93	11.64	10.38	22.26	48.17
25	3.71	6.14	10.38	25.52	50.55
26	3.20	9.42	8.86	19.45	48.27
27	3.98	14.73	17.53	41.38	50.32
28	4.73	22.35	22.90	60.25	67.27
29	4.01	14.74	13.75	29.87	61.88
30	2.71	11.08	9.85	21.05	66.68
31	·/.	·/.	·/.	·/.	50.02

Radioactivity pc/m^3

June 1977	fallout $.10^{-2}$	Be7 $.10^{-2}$	P32 $.10^{-3}$	P33 $.10^{-3}$	O_3 ppb
1	3.55	14.19	9.06	21.46	47.17
2	2.14	9.29	7.40	17.78	44.30
3	1.89	7.57	6.68	14.31	52.04
4	2.04	4.89	4.79	9.11	54.00
5	1.54	6.49	5.45	10.76	50.08
6	2.08	2.44	1.37	1.36	45.00
7	1.86	6.86	5.09	9.66	48.98
8	1.96	6.87	6.07	10.63	46.01
9	2.79	8.23	5.68	12.44	39.47
10	2.45	6.80	3.32	8.46	32.28
11	2.37	9.00	3.76	8.79	38.92
12	2.75	12.32	7.50	13.14	41.44
13	3.15	11.62	7.08	11.33	37.97
14	0.74	2.42	1.07	2.57	41.38
15	0.10	0.13	0.19	0.41	37.78
16	1.00	4.53	4.40	10.48	50.54
17	2.54	4.60	4.90	9.31	52.45
18	2.77	7.07	6.44	14.33	49.27
19	1.59	4.37	5.90	12.31	38.00
20	1.42	5.09	5.54	11.60	37.92
21	1.41	2.84	4.60	9.52	44.11
22	1.97	4.14	5.67	13.60	42.38
23	2.54	7.51	7.88	12.84	54.26
24	2.73	8.30	8.55	16.03	60.96
25	0.89	8.15	3.22	5.37	56.60
26	0.29	1.10	1.26	2.52	50.72
27	1.73	7.02	8.15	16.94	48.03
28	3.35	8.02	10.18	17.63	53.12
29	1.20	2.89	2.79	4.16	50.27
30	0.90	3.84	3.74	6.93	54.65

Radioactivity pc/m^3

July 1977	fallout $.10^{-2}$	Be7 $.10^{-2}$	P32 $.10^{-3}$	P33 $.10^{-3}$	O_3 ppb
1	3.65	4.50	3.60	3.39	49.92
2	3.42	4.25	3.20	3.28	44.11
3	2.84	5.69	4.61	5.23	49.67
4	2.53	7.06	5.97	6.28	56.03
5	3.09	10.56	7.57	12.02	60.61
6	2.92	8.91	9.88	16.68	60.00
7	3.51	9.47	8.14	9.87	60.74
8	1.94	5.54	4.94	8.25	56.04
9	0.63	1.80	1.91	2.59	60.85
10	1.66	4.82	5.50	10.72	63.33
11	2.62	10.17	12.03	13.84	62.27
12	3.82	9.79	*/.	*/.	56.29
13	3.37	10.38	*/.	*/.	58.04
14	1.12	3.40	*/.	*/.	52.67
15	2.39	8.80	*/.	*/.	50.42
16	2.44	10.06	*/.	*/.	56.41
17	2.16	7.80	*/.	*/.	55.86
18	3.02	11.14	*/.	*/.	50.72
19	2.24	9.15	*/.	*/.	43.80
20	1.06	5.55	*/.	*/.	44.47
21	1.56	10.51	*/.	*/.	44.40
22	1.59	11.33	*/.	*/.	54.67
23	1.38	7.99	*/.	*/.	41.95
24	1.97	7.78	*/.	*/.	48.83
25	1.02	3.43	*/.	*/.	41.11
26	0.51	2.00	*/.	*/.	35.28
27	1.15	6.40	*/.	*/.	43.72
28	1.35	8.59	*/.	*/.	46.85
29	1.64	8.30	*/.	*/.	46.92
30	0.98	5.79	*/.	*/.	50.14
31	0.68	1.41	*/.	*/.	53.57

Radioactivity pc/m^3

Aug 1977	fallout $.10^{-2}$	Be7 $.10^{-2}$	P32 $.10^{-3}$	P33 $.10^{-3}$	O_3 ppb
1	0.57	0.20	·/.	·/.	47.79
2	1.12	6.75	·/.	·/.	48.36
3	2.09	12.41	·/.	·/.	49.60
4	1.59	11.36	·/.	·/.	50.58
5	1.80	7.88	·/.	·/.	68.25
6	2.67	10.60	·/.	·/.	64.23
7	2.72	10.89	·/.	·/.	52.02
8	2.05	11.09	·/.	·/.	49.59
9	0.85	4.09	·/.	·/.	51.30
10	0.96	5.33	·/.	·/.	55.45
11	4.68	10.52	·/.	·/.	49.26
12	4.35	12.78	·/.	·/.	51.51
13	2.03	5.43	·/.	·/.	54.08
14	1.76	6.70	·/.	·/.	52.60
15	6.13	6.53	·/.	·/.	52.06
16	2.74	5.03	·/.	·/.	46.58
17	3.58	5.36	·/.	·/.	41.46
18	1.11	3.09	·/.	·/.	44.51
19	·/.	1.51	·/.	·/.	40.15
20	·/.	5.01	·/.	·/.	40.18
21	·/.	0.02	·/.	·/.	37.17
22	·/.	4.60	·/.	·/.	47.28
23	·/.	3.27	·/.	·/.	53.33
24	·/.	2.44	·/.	·/.	49.90
25	·/.	3.06	·/.	·/.	41.45
26	·/.	4.09	·/.	·/.	44.58
27	·/.	4.40	·/.	·/.	45.69
28	·/.	3.46	·/.	·/.	39.36
29	·/.	5.03	·/.	·/.	34.36
30	·/.	7.25	·/.	·/.	38.92
31	2.09	7.84	·/.	·/.	39.61

Radioactivity pc/m^3

Sep 1977	fallout $.10^{-2}$	Be7 $.10^{-2}$	P32 $.10^{-3}$	P33 $.10^{-3}$	O_3 ppb
1	1.89	6.35	*/.	*/.	41.52
2	2.45	7.50	*/.	*/.	42.28
3	1.88	5.98	*/.	*/.	50.66
4	2.15	9.83	*/.	*/.	*/.
5	2.04	8.16	*/.	*/.	*/.
6	1.81	9.02	*/.	*/.	46.35
7	1.46	6.71	*/.	*/.	33.65
8	1.20	4.31	*/.	*/.	26.76
9	0.72	6.13	*/.	*/.	35.63
10	1.69	8.68	*/.	*/.	31.28
11	1.19	4.64	*/.	*/.	24.62
12	1.59	5.92	*/.	*/.	31.99
13	1.55	10.41	*/.	*/.	*/.
14	1.69	5.42	*/.	*/.	*/.
15	1.25	5.63	*/.	*/.	*/.
16	1.34	6.01	*/.	*/.	*/.
17	0.85	2.41	*/.	*/.	*/.
18	0.56	0.80	*/.	*/.	*/.
19	1.01	2.80	*/.	*/.	*/.
20	1.48	6.07	*/.	*/.	27.46
21	1.28	3.87	*/.	*/.	26.70
22	1.79	6.23	*/.	*/.	25.22
23	0.78	4.73	*/.	*/.	19.25
24	2.20	6.94	*/.	*/.	22.98
25	0.63	3.12	*/.	*/.	21.30
26	0.57	2.13	*/.	*/.	35.21
27	1.35	8.07	*/.	*/.	38.94
28	4.56	8.70	*/.	*/.	37.38
29	50.39	10.05	*/.	*/.	32.72
30	59.20	17.24	*/.	*/.	35.51

Radioactivity pc/m^3

Oct 1977	fallout $.10^{-2}$	Be7 $.10^{-2}$	P32 $.10^{-3}$	P33 $.10^{-3}$	O_3 ppb
1	43.08	14.45	*/.	*/.	35.50
2	2.64	5.41	*/.	*/.	*/.
3	19.65	8.17	*/.	*/.	*/.
4	56.40	19.54	*/.	*/.	38.98
5	28.64	7.81	*/.	*/.	38.10
6	5.76	2.55	*/.	*/.	33.03
7	8.42	8.65	*/.	*/.	27.20
8	3.12	4.85	*/.	*/.	26.65
9	14.33	12.45	*/.	*/.	25.51
10	0.56	0.77	*/.	*/.	28.03
11	1.20	1.27	*/.	*/.	29.66
12	3.71	3.62	*/.	*/.	34.47
13	10.41	7.88	*/.	*/.	44.37
14	17.37	21.63	*/.	*/.	43.58
15	10.44	8.32	*/.	*/.	39.38
16	15.02	14.28	*/.	*/.	38.69
17	9.51	19.70	*/.	*/.	37.29
18	8.36	29.80	*/.	*/.	40.39
19	8.84	22.33	*/.	*/.	38.46
20	6.56	16.28	*/.	*/.	37.34
21	3.85	8.39	*/.	*/.	29.29
22	3.82	13.63	*/.	*/.	31.91
23	5.41	12.75	*/.	*/.	38.42
24	2.86	12.01	*/.	*/.	33.30
25	3.65	12.38	*/.	*/.	31.64
26	2.56	11.84	*/.	*/.	30.67
27	4.65	13.30	*/.	*/.	30.82
28	1.46	9.24	*/.	*/.	34.54
29	3.02	12.39	*/.	*/.	39.22
30	4.20	16.36	*/.	*/.	38.93
31	4.12	14.45	*/.	*/.	38.33